

Fall 12-16-2016

Factors affecting algal biomass growth and cell wall destruction

Alicia E. Simosa
aesimosa@uno.edu

Follow this and additional works at: <https://scholarworks.uno.edu/td>



Part of the [Environmental Engineering Commons](#)

Recommended Citation

Simosa, Alicia E., "Factors affecting algal biomass growth and cell wall destruction" (2016). *University of New Orleans Theses and Dissertations*. 2277.
<https://scholarworks.uno.edu/td/2277>

This Thesis-Restricted is protected by copyright and/or related rights. It has been brought to you by ScholarWorks@UNO with permission from the rights-holder(s). You are free to use this Thesis-Restricted in any way that is permitted by the copyright and related rights legislation that applies to your use. For other uses you need to obtain permission from the rights-holder(s) directly, unless additional rights are indicated by a Creative Commons license in the record and/or on the work itself.

This Thesis-Restricted has been accepted for inclusion in University of New Orleans Theses and Dissertations by an authorized administrator of ScholarWorks@UNO. For more information, please contact scholarworks@uno.edu.

Factors affecting algal biomass growth and cell wall destruction

A Thesis

Submitted to the Graduate Faculty of the
University of New Orleans
in partial fulfillment of the
requirements for the degree of

Master of Science
in
Engineering
Civil and Environmental

by

Alicia Eugenia Simosa Mellado

B.S. Civil Engineering
Universidad Católica Andres Bello
Puerto Ordaz – Bolivar, Venezuela, 2014

December 2016

Copyright 2016, Alicia E. Simosa M.

Dedication

To my mother,
Victoria Mellado,
for her effort, support, guidance and dedication,
to help me achieve this goal.

To all my family,
especially to my brother and sister, Juan and Victoria,
and my uncle, Jose Carlos Simosa,
for their unconditional support.

To my fiancé, Luis Perez,
whose love, patience and support,
helped me overcome every obstacle
and motivated me to keep going at all times.

Acknowledgments

I am grateful with The Jefferson Parish Department of Sewerage for funding my Master's Program through a Research Assistantship.

I am immensely grateful to Dr. Enrique La Motta, for giving me the opportunity to work with him, for believing in me, for helping me, for his unconditional support and for guiding me every step during this Master's degree program.

I would like to thank Dr. Guillermo Rincon for his valuable assistance during this research project.

I would also like to thank Dr. Miguel Guevara and the Microalgae Laboratory of the Oceanographic Institute of Venezuela for their help in the laboratory experiments performed in this research.

My gratitude to my friend and colleague Jessica Simpson for her invaluable support and help.

Also, I would like to specially thank all my friends, Adrian Ballabriga, Luis Meneses, Anibal Hernandez, Irma Salazar, Ruth Deffit, Yolyamar Montes De Oca, Laura Andrade, Daniela de Leon, Marcos Montes de Oca, Naomi Boada, Rama Hbos and Luis De Grau, who even in the distance, emotionally helped and supported me.

Table of Contents

List of Symbols and Abbreviations	viii
List of Figures	ix
List of Tables	xi
Abstract	xii
Chapter I: Introduction.....	1
Chapter II: Literature Review.....	4
<i>Chlorella Vulgaris</i>	4
Kinetics of growth	6
Logistic growth curve	7
Batch Culture Techniques for algae cultivation	8
Microalgae Culture Systems	9
a. Open systems	9
b. Closed systems.....	10
c. Hybrid culture systems.....	14
d. Heterotrophic culture systems	14
Factors influencing the growth of microalgae.....	15
a. Light.....	15
b. Nutrients.....	16
c. pH.....	17
d. Agitation	19
e. Temperature	19
Effect of CO ₂ on pH.....	19
Effect of CO ₂ in algal growth.....	21
Buffering capacity of water	22
Recuperation, fixation and transformation of CO ₂ into biomass	22
Electroporation	26
a. Basics and mechanisms.....	26
b. Irreversible Electroporation.....	28
Conversion of algal biomass to biofuel	29
a. Lipids	31
b. Stages of biomass production.....	33

c. Economic Feasibility of microalgae biodiesel.....	35
Wastewater treatment using microphytes and macrophytes	36
Chapter III: Laboratory Equipment and Experimental Set-up	40
Laboratory equipment.....	40
a. Shaking water bath	40
b. Electrochemical batch reactor.....	42
Laboratory methods.....	44
a. Medium preparation for algae growth	44
b. pH	45
c. Conductivity.....	45
d. Alkalinity	45
e. Calcium	45
f. Turbidity	46
g. Chlorophyll A	46
h. Cell wall break.....	46
Experiment design.....	47
a. Experiment 1: Algae cultivation under a CO ₂ percentage range from 0 to 20%.....	47
b. Experiment 2: Growth of a large volume of algae using the optimum CO ₂ concentration found in experiment 1.	50
c. Experiment 3: Irreversible electroporation of algae cell wall.	51
Chapter IV: Results and Data Analysis	52
Experiment 1.....	52
a. Turbidity	52
b. pH	61
c. Alkalinity measurements.....	62
d. Chlorophyll A measurements	63
e. Correlation between turbidity and chlorophyll a concentration	64
Experiment 2.....	65
Experiment 3.....	66
a. Electroporation experiment using constant voltage	66
b. Electroporation using constant current	70
Chapter V: Conclusions and Recommendations.....	74
Conclusions	74

Recommendations	75
Chapter VI: References.....	77
Chapter VII: Appendix	81
Appendix A: Detailed explanation of laboratory methods.	81
a. Medium preparation for algae growth	81
b. pH and Conductivity	83
c. Alkalinity	87
d. Calcium	89
e. Turbidity.....	91
f. Chlorophyll A	93
g. Cell wall break.....	96
Appendix B: Experimental results.	99
Vita	110

List of Symbols and Abbreviations

$\{H^+\}$: Hydrogen ion activity

Alk: Alkalinity, mg/L as $CaCO_3$

Ca: Calcium, mg/L as $CaCO_3$

CO_2 : Carbon dioxide

CO_3^{2-} : Carbonate

HCO_3^- : Bicarbonate

$H_2CO_3^*$: Carbonic acid or carbon dioxide (aqueous)

NTU: Nephelometric Turbidity Unit

OH^- : Hydroxide

PC: Proton condition

PRL: Proton reference level

List of Figures

Figure 1. <i>Chlorella vulgaris</i> . SOURCE: www.harmonicarts.ca	5
Figure 2. Growth phase diagram. SOURCE: www.fao.org	7
Figure 3. Raceways ponds. SOURCE: www.aban.com	10
Figure 4. Algae chamber. SOURCE: www.flickr.com	11
Figure 5. Tubular photobioreactor. SOURCE: www.bbi-biotech.com	12
Figure 6. Vertical photobioreactor. SOURCE: University of Kentucky. Center for Applied Energy Research (CAER). Department of Biosystems & Agricultural Engineering (BAE).	13
Figure 7. Photobioreactor internally illuminated. SOURCE: American Society of Mechanical Engineers (ASME).	14
Figure 8. H_2CO_3^* PRL	18
Figure 9. Log concentration diagram of a 10^{-3}CO_2 solution. SOURCE: www.chem.libretexts.org	20
Figure 10. Buffer capacity of a natural water with total carbonic species concentration of 0.01 mol/L. SOURCE: Dr. Enrique La Motta's ENCE 6313 class notes.	22
Figure 11. Light-dependent reactions harness energy from the sun to produce ATP and NADPH. SOURCE: "The Calvin cycle: Figure 1," by OpenStax College, Concepts of Biology CC BY 4.0.....	23
Figure 12. Calvin-Benson cycle. "The Calvin cycle: Figure 2," by OpenStax College, Concepts of Biology CC BY 4.0	25
Figure 13. Cell in an electric field. (Electroporated area is presented with dashed line). SOURCE: (Kanduser, 2009).....	27
Figure 14. Irreversible electroporation. SOURCE: www.intechopen.com	29
Figure 15. US energy consumption by energy source, 2015. SOURCE: U.S. Energy Information Administration, Monthly Energy Review, Table 1.3 and 10.1 (April 2016), preliminary data.	30
Figure 16. Process of obtaining oil from microalgae. SOURCE: (Malgas, 2013).....	34
Figure 17. AIWSP system. SOURCE: www.stabilizationponds.sdsu.edu	38
Figure 18. Shaking water bath.	40
Figure 19. Flasks used in the experiments. (a) Experiment 1, (b) Experiment 2.....	41
Figure 20. Flask arrangement (first part).	41
Figure 21. Electrochemical batch reactor.	42
Figure 22. Electrode and spacer dimensions. SOURCE: (Rincon, 2013).....	43
Figure 23. Cell arrangement. SOURCE: (Rincon, 2013).	43
Figure 24. Opening for gas exit. SOURCE: (De Grau, 2015).....	44
Figure 25. <i>Chlorella Vulgaris</i> culture.	47
Figure 26. Experiment 1 set up, showing the connections between the flasks, air supply and CO_2 cylinder.	49
Figure 27. Experiment 2 set up, showing the bottle inside the water bath and the flasks interconnected to prevent evaporation.	50
Figure 28. One cell batch reactor.....	51
Figure 29. Non-linear regression plot for flask 0.	54
Figure 30. Algae growth from start to end for flask 0.....	55
Figure 31. Non-linear regression plot for flask 1.	55

Figure 32. Algae growth from start to end for flask 1.....	56
Figure 33. Clumps in the bottom of flask 1 for days 21 and 40.....	56
Figure 34. Non-linear regression plot for flask 2.	57
Figure 35. Algae growth from start to end for flask 2.....	58
Figure 36. Clumps in the bottom of flask 2 for days 16 and 30.....	58
Figure 37. Non-linear regression plot for flask 3.	59
Figure 38. Algae growth from start to end for flask 3.....	60
Figure 39. Non-linear regression plot for flask 4.	60
Figure 40. Algae growth from start to end for flask 4.....	61
Figure 41. Correlation between turbidity and chlorophyll a concentration.	64
Figure 42. Gases and water vapor.	72
Figure 43. Bristol's Algae Media.	82
Figure 44. Well-mixed medium.	82
Figure 45. Buffer solutions for pH meter.	84
Figure 46. Orion Star™ Plus Meter.....	84
Figure 47. Thermo Orion pH meter.....	86
Figure 48. Conductivity calibration standards.....	86
Figure 49. Conductivity probe.	87
Figure 50. Alkalinity indicator end point (Pink).	89
Figure 51. Calcium indicator end point (Blue).	91
Figure 52. Turbidimeter.....	92
Figure 53. Turbidimeter calibration set.	92
Figure 54. Filtering Apparatus completely assembled.....	94
Figure 55. Tubes with filter and acetone.	95
Figure 56. Samples inside the centrifuge.	95
Figure 57. Cell wall analysis equipment.	99

List of Tables

Table 1. Oil content of some microalgae species. SOURCE: (Malgas, 2013)	32
Table 2. Characteristics of Microalgae Harvesting Techniques. SOURCE: (Biofuels, 2012)	33
Table 3. CO ₂ percentage and flow rate.	48
Table 4. Readings using air flow rotameter to get desired CO ₂ flow rate.	49
Table 5. Turbidity results.	52
Table 6. Alkalinity results.	63
Table 7. Alkalinity trial.	63
Table 8. Chlorophyll concentration.	64
Table 9. Exhaust gases composition by volume (%v/v). SOURCE: (The k2p blog, 2013) www.ktwop.com.....	65
Table 10. Constant voltage mode results.	66
Table 11. Constant current mode results.	70
Table 12. Temperature results.	72
Table 13. pH values for flask 3.	99
Table 14. Non-linear regression on data turbidity vs. time for flask 0.	100
Table 15. Non-linear regression on data turbidity vs. time for flask 1.	100
Table 16. Non-linear regression on data turbidity vs. time for flask 2.	101
Table 17. Non-linear regression on data turbidity vs. time for flask 3.	102
Table 18. Non-linear regression on data turbidity vs. time for flask 4.	103
Table 19. Correlation between turbidity and chlorophyll concentration.....	103
Table 20. Daily measurements.	104
Table 21. Algae culture progress.	108

Abstract

Research using microalgae *Chlorella vulgaris* was conducted in order to determine the maximum CO₂ concentration under which algae can grow, within the emission range from oil and natural gas burning plants (0-20%).

After choosing the optimal CO₂ percentage, pH and alkalinity were determined; and finally, an electrochemical (EC) batch reactor connected to DC current was applied to achieve algae cell annihilation, and therefore, facilitate anaerobic digestion, methane production and energy recovery.

It was determined that algae can grow under 20% CO₂, being 15% CO₂ the most effective (pH of 6.64 and alkalinity of 617.5 mg/L CaCO₃).

Electroporation using an electrochemical batch reactor is effective in breaking cells membranes, which simplifies anaerobic digestion process and methane production.

The parameters found effective for completely breaking the algae cell are: detention time of 1 ± 0.5 minutes, and minimum voltage and current of $65 \frac{\text{Volts}}{285 \text{ ml}}$ and $3.9 \frac{\text{Amps}}{285 \text{ ml}}$, respectively.

Keywords: Algae, *Chlorella vulgaris*, CO₂ emissions, biomass, biofuel, electroporation, cell wall, CO₂ neutralization, CO₂ recycling, electrocution of algae cells, algae cell membrane fracture, algae biofuel, electrochemical algae treatment.

Chapter I

Introduction

One of the biggest threats hanging over our planet is climate change, caused primarily by the emission of greenhouse gases, which come mainly from fuels (oil, gas and coal) burned in electric power generation, heating, cooling, and transportation. Of all greenhouse gases being generated, the most important one is CO₂, which comes from emissions from large industry and deforestation of tropical and subtropical forests by the irrational expansion of agricultural, agro-industrial and forestry activities (Madrid, 2009).

Studies indicate that between 1990 and 2012 has been an increase of 67% in CO₂ emissions from coal (EIA, 2016).

Meeting this increasing demand for energy without increasing CO₂ emissions requires more than a mere increase in energy production efficiency. The situation requires a comprehensive plan to more efficiently utilize all of the existing sources for energy while sequestering, capturing, and storing the carbon emitted through the global energy system. Carbon Capture and Storage (CCS) could play a major role in reducing atmospheric CO₂ emissions through efficient and responsible fossil fuel usage and recycling (Karcher, 2010).

Bioenergy production from microalgae was contemplated since the fifties. The economic potential of this technology was recognized by several countries such as USA, Japan and Australia especially after the energy crisis in 1975 (Arredondo, 1991). In the years 1990-2000 the Japanese government used a program to study CO₂ fixation and optimization of microalgal growth. However, these projects were suspended in part, due to the lack of competitiveness of biofuel to fossil fuel prices (Malgas, 2013).

The use of microalgae for biodiesel production is an advantageous alternative due to the high lipid content and suitable profile for obtaining biofuels they offer. In addition to this, other attributes of microalgae are its high photosynthetic efficiency, their ability to grow both in marine and brackish water, fresh water, and wastewater, and its relatively high rate of growth and ease to control carbon emissions by absorbing and fixing large amounts of CO₂ during cultivation. Based on mass balance, the carbon dioxide sequestration value can be quantified as follows: for every kg of algae biomass created, 1.83 kg of CO₂ are sequestered (Chisti, 2007).

However, systems of cultivation of microalgae currently have certain limitations such as the lack of information for scaling, difficulty maintaining monocultures, high operating costs for the production and harvesting of the biomass of microalgae, among others (Malgas, 2013).

Today, it is possible to dry the biomass of algae and burn it directly for heat and electricity generation, or to perform high temperature and high pressure processes, such as pyrolysis, gasification and hydrothermal improvement (HTU) to produce fuel in the form of gas or liquid, respectively. These processes require dry biomass. The drying process requires a lot of energy, which has a negative effect on the energy balance of the process and the costs of the necessary equipment (Wijffels, 2010).

A biochemical technology to process biomass is anaerobic digestion. This produces biogas from wet stream and requires less energy than thermochemical processes. The biogas contains between 55 and 75% of methane, which can be burned for heat and/or electricity, and can be upgraded to replace natural gas (Garcia, 2010).

Methane generation from waste CO₂ emissions is an attractive alternative to recover fuel for gas-fired power plants. Energy recovery from waste CO₂ emissions combined with municipal wastewater would help reduce traditional fuel consumption, and would result in the reduction of conventional wastewater treatment needs, and recycling spent CO₂. Methane reuse as a fuel by gas-fired power plants would also translate into lower greenhouse gas (GHG) emissions.

Although conversion of harvested algae to methane by anaerobic digestion was suggested in the late 1950s (Golueke, 1956), it was found that the algae cell wall remained intact after anaerobic digestion, which resulted in lower methane yield. If this objection could be removed by achieving algae cell destruction through electro-coagulation/electro-annihilation (ECE), high-rate anaerobic digestion of harvested algae becomes an effective option for energy recovery. ECE offers many advantages over conventional chemical coagulation, including the destruction of algal cells by the electro-chemical processes taking place in the EC batch reactor.

Anaerobic digestion is a robust and well developed technology. This technology is applied to wastes containing organic compounds, with the very low price of raw materials. Given the limitations of other processes of cell treatment, anaerobic digestion appears more feasible (FAO, 2009).

For this research, the microalgae *Chlorella vulgaris* was chosen due to several characteristics of this algae species: its high lipid percentage, its easy reproduction and growth, adaptation to any media, its high percentage of absorption and fixation of CO₂ and its ability to work under a wide range of temperature and pH. The initial objective of this research is to determine the maximum CO₂ concentration that can be added to the suspension of algae by growing them in a medium containing a CO₂ range of 0 to 20% for several weeks; this range was chosen because petroleum-burning plants emit a maximum of 15% CO₂, and plants that burn natural gas (methane), emit less than half, i.e., between 6 and 7% (EIA, 2016); therefore, all CO₂ emissions ranges that can be sequestered, are being studied.

The next objective is to define the optimal pH and alkalinity for maximum growth, and finally, apply electrochemical processes using an EC batch reactor to achieve algae cell annihilation, which facilitates the process of anaerobic digestion by wastewater treatment plants and makes it more effective for methane production, which in turn leads to efficient energy recovery. The electrochemical cell configuration and detention time required for irreversible electroporation of cell membrane were also determined.

Chapter II

Literature Review

The purpose of this chapter is to provide the theoretical foundations on which this research is based. First, a discussion about the microalgae used, their growth, cultivation techniques, different types of existing systems and principal factors affecting their growth are discussed. Then, an analysis of the buffering capacity of the water and the effect that CO₂ has in both the pH and the growth of algae is also presented. The chapter continues with a detailed analysis of the complete process of transformation of CO₂ to biomass and then to biofuel, with emphasis on the cycles and processes necessary to perform it. Finally, the economic viability of microalgae biofuel and wastewater treatment using algae is briefly introduced.

Chlorella Vulgaris

Chlorella vulgaris is a unicellular green alga belonging to the protist kingdom. It is spherical, with a diameter of 2 to 10 µm, it has no flagellum and it is present in most freshwater bodies. *Chlorella* contains the green photosynthetic pigments, chlorophyll a and b in its chloroplast. Through photosynthesis it multiplies rapidly, requiring only sunlight, carbon dioxide, water and small amounts of minerals dioxide (Safi, 2014).

Chlorella Vulgaris is probably one of the first organisms that arose on Earth, dating back at least 540 million years ago. Their cells have the ability to adapt to major climate changes and can grow in different environments of pH and temperature. His remarkable survival is due to one fundamental characteristic:

- Almost unbreakable cell wall which is able to coexist in places with high concentrations of pesticides, toxins and heavy metals.

Chlorella took a boom in the 40s due to its high proportion of protein and other essential nutrients for humans. The most recognizable feature is its very comparable photosynthetic efficiency with other highly efficient crops. In addition, when dried contains about 45% protein, 20% fat, 20% carbohydrate, 5% fiber, 10% minerals and vitamins (Safi, 2014).

The use of microalgae for the purification of wastewater has been promoted since the late fifties by Oswald (1957). Likewise, in the 70s, open microalgae culture systems for wastewater treatment were developed in the US in which the biomass obtained was transformed to methane (Ugwu, 2008). However, this treatment system has been hampered due to the large area of land needed and the use of other treatment systems such as activated sludge.

Stabilization ponds are used today in many parts of the world for wastewater treatment, especially in developing countries (Mara, 1998). The ability of the algae to remove both nitrogen and phosphorus from wastewater, among others, represents a real possibility for removing nutrients from wastewater, showing that phosphorus removal can be as efficient as the conventional chemical treatment (Hoffman, 1998). Its main advantages are lower cost, since chemicals are not necessary, and the recovery of nutrients in form of biomass which can be used as fertilizer.

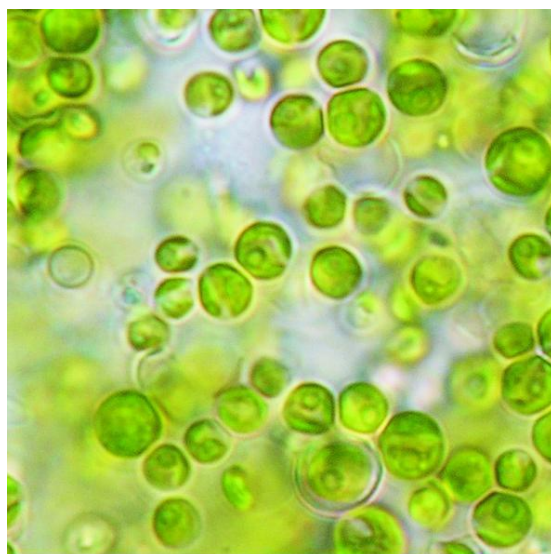


Figure 1. *Chlorella vulgaris*. SOURCE: www.harmonicarts.ca

There is a great potential in the combination of processes involving microalgae, such as obtaining biodiesel from microalgae, or anaerobic digestion of the microalgae for obtaining methane (Malgas, 2013). Combining the production of microalgae and wastewater treatment, significant savings in the consumption of nutrients occurs.

Kinetics of growth

Algae, as well as many other microorganisms, grow following several phases (see figure 2) (Karcher, 2010):

- **Lag phase (1):** Algae adapt to new medium. Growth progresses slowly.
- **Exponential or logarithmic phase (2):** Algae have adapted to their surroundings. The increment in algal biomass per time is proportional to the biomass in the population at any given point in time according to the equation:

$$\frac{dn}{dt} = rN \quad (1)$$

the solution to which is:

$$N_t = N_0 e^{rt} \quad (2)$$

where r is the exponential growth rate of the population, N_t is the population at time t , and N_0 is the initial population.

- **Declining growth phase (3):** Growth has occurred to such an extent that superposing of cells occurs and nutrients become limited. This effect reduces the growth rate and the increase in algal biomass becomes linear. This phase concludes when respiration outweighs photosynthesis, nutrients become deficient, or toxic waste buildup in the sample becomes significant.

- **Stationary phase (4):** Rate of growth is equal to the rate of dead. Maximum attainable concentration of algal biomass in the specified closed system. Dead algae serve as food.
- **Death phase (5):** Mark increasing cell death and disappearance of cells.

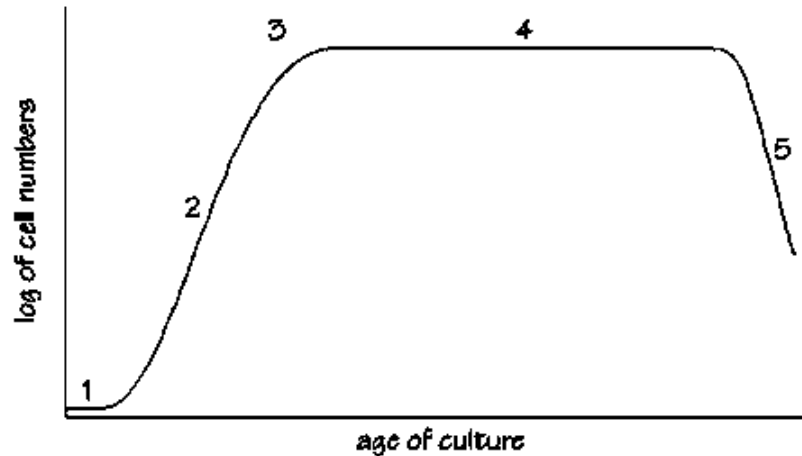


Figure 2. Growth phase diagram. SOURCE: www.fao.org

Logistic growth curve

Logistic growth curve is an S-shaped (sigmoidal) curve that can be used to model functions that increase gradually at first, more rapidly in the middle growth period, and slowly at the end, leveling off at a maximum value after some period of time. The initial part of the curve is exponential; the rate of growth accelerates as it approaches the midpoint of the curve. At the midpoint, the growth rate begins to decelerate but continues to grow until it reaches an asymptote, X_{max} which is called the "Carrying Capacity" for the environment.

This type of curve is frequently used to model biological growth patterns where there is an initial exponential growth period followed by a leveling off as more of the population is infected or as the food supply or some other factor limits further growth.

The equation of the logistic growth curve is the following:

$$X = \frac{X_{max}}{1 + me^{-nt}} \quad (3)$$

Where:

X = Predicted Y value.

Xmax = Maximum attainable concentration of algal biomass (Asymptote).

m = Parameter that defines the curvature of the logistic growth curve.

n = Rate of growth.

R² = Degree of goodness of fit.

The values of the best-fit parameters, Xmax, m, and n, were found using Excel Solver, by minimizing the sum of the squares of the residuals, defined by Eq. 4:

$$SS_{res} = \sum_i (y_i - f_i)^2 = \sum_i (e_i)^2 \quad (4)$$

The value of the coefficient of determination, R², was found using Eq. 5:

$$R^2 = 1 - \frac{SS_{res}}{SS_{tot}} \quad (5)$$

Where:

$$SS_{tot} = \sum_i (y_i - \bar{y})^2 \quad (6)$$

Batch Culture Techniques for algae cultivation

When bio-fuels production or maximum carbon sequestration is the goal, maintenance of the algal suspension in the exponential growth phase is critical, because this is the phase where growth rate is calculated. The increment in algal biomass per time is proportional to the biomass

in the population. As Becker (1994) describes, during this phase a steady-state continuum is observed and the plot of the logarithm of cell mass yields a linear increase with time.

There are multiple ways to accomplish this task; however, they all involve replacement with fresh medium. The method has been practiced since culturing began and is generally accepted as the standard method. It involves culturing the suspension into the exponential growth phase, then removing a portion of the culture and replacing with fresh medium. Wood et al. (2005) describe this simple process, the goal of which is to ensure the medium remains fresh and the algae in the culture never have to compete with each other for resources. This allows for continuous exponential growth and harvesting of cells (Karcher, 2010).

Microalgae Culture Systems

Microalgae culture systems are usually classified according to their configuration and type of operation:

a. Open systems

They can be classified in turn as natural surface water (ponds, lagoons and lakes) and artificial ponds. Artificial systems have different designs: inclined (thin film), circular carousel ponds or channels (raceway ponds).

The channels or "raceway ponds" generally are concrete shallow oval channels (15-20 cm), in form of a closed circuit, where the crop is recirculated and mixed to promote the stabilization of growth and productivity of microalgae (see figure 3). Due to the shallow depth of the channels, diffusion from the atmosphere allows algae to obtain the CO₂ needed for growth.

Production through ponds or lagoons is cheaper compared with the photobioreactors (discussed later), both in investment and in maintenance and energy consumption during operation method.

However, in a system of open culture it is difficult to maintain a single species of microalgae, due to the ease of biological contamination, which can even assume that crop infection by bacteria or other microorganisms (Malgas, 2013).



Figure 3. Raceways ponds. SOURCE: www.aban.com

b. Closed systems

Closed systems are in total isolation with the outside environment and therefore without direct contact with the atmosphere. This total isolation from the external environment represents a total reduction of pollution, greater control of growing conditions and generally higher returns (Malgas, 2013).

Algae Chambers

Algae chambers are closed systems of small-scale production (Figure 4) in which the culture volume increases. Containers of various sizes are used to maintained the culture under

very controlled conditions of temperature, light, among others. Temperature control is performed by means of thermostats (Malgas, 2013).



Figure 4. Algae chamber. SOURCE: www.flickr.com

Photobioreactors

A photobioreactor is a tightly closed system for obtaining further growth of the desired microalgae. Photobioreactors are characterized by the regulation and control of the most important parameters of growth, while reducing the risk of contamination and loss of CO₂ diffusion.

They can be classified according to their design and mode of operation (Malgas, 2013):

- From the point of view of design, the photobioreactors can be classified as: (a) flat or tubular, (b) horizontal, vertical, inclined or spiral, (c) coils (pipe bends, serial flow) or (d) multiple (parallel flow from a delivery collector at a collector).

- From the point of view of the operation mode, the photobioreactors can be classified as: (a) driven agitated by air or pumps, (b) reactors phase (gas exchange occurs in a separate chamber) or (c) two phase reactors (there is gas exchange chamber, but it is produced throughout the reactor).

Closed photobioreactors that are being highly investigated for application to the commercial production of algae with high added value include:

- **Tubular photobioreactors:** one of the most suitable photobioreactors for cultivation outdoors, because of their high ratio lit are/reactor volume (Figure 5). Mass transfer and the degree of agitation in the tubular photobioreactors are limited, causing high concentrations of O₂.



Figure 5. Tubular photobioreactor. SOURCE: www.bbi-biotech.com

- **Flat walls photobioreactors, inclined or vertical:** formed by two sheets of transparent materials generally plastic (rigid or flexible) vertical or inclined, between which the culture is stirred by mechanical or pneumatic systems.

The space between the plates is usually between 1 and 20 cm, and the height thereof up to 2 m. They have the advantage of enabling large crop areas exposed to light per unit area of land. Dissolved O₂ concentrations are low and photosynthetic efficiencies that are achieved are high (Malgas, 2013).

- **Vertical column photobioreactors:** consist of a standpipe height generally between 1 and 3 m, and a diameter ranging between 5 and 500 cm, wherein air is bubbled from the bottom (Ugwu C. A., 2007) as agitation system. They are compact and inexpensive, and very easy to sterilize (Figure 6).



Figure 6. Vertical photobioreactor. SOURCE: University of Kentucky. Center for Applied Energy Research (CAER). Department of Biosystems & Agricultural Engineering (BAE).

- **Photobioreactors internally illuminated:** interior lighting of photobioreactors can be natural, by using fiber optics and solar collectors that collect sunlight outside and transferred into the reactor, or may be artificially by fluorescent lamps (Figure 7) (Malgas, 2013).



Figure 7. Photobioreactor internally illuminated. SOURCE: American Society of Mechanical Engineers (ASME).

c. Hybrid culture systems

Hybrid culture systems combine different stages of growth in photobioreactors and open lagoons or ponds. Generally, these systems consist of a first stage of production of biomass in photobioreactors, where greater control of environmental conditions, minimizing contamination and maximizing cell division take place. In the second stage, microalgae are grown in open ponds for accumulation of the products induced by nutrient deficiency in the system, like wastewater effluents from pig farms and municipal waste, or in some cases, seawater or water with high salinity (Brendan, 2010).

d. Heterotrophic culture systems

A significant number of microalgae is able to grow in the absence of light, using organic carbon substrates, such as glucose. Algae cultivation is performed in stirred closed bioreactors,

in an adaptation of fermentation technology. These are systems that allow easy change of scale and generate the highest density of biomass produced. Also, they provide a high degree of growth control and reduced harvest costs, but have a higher energy consumption (Borowitzka, 1999).

Factors influencing the growth of microalgae

The following factors have been identified to influence microalgae growth (Malgas, 2013):

a. Light

The availability of light is the main limiting factor of microalgae growth. Inorganic nutrients, and even CO₂, can be incorporated into the culture medium in excess, so that they will never be growth limiting.

Photosynthetic organisms employ only the fraction of the sunlight spectrum that is photosynthetically active, that is, between 350 and 700 nm. Microalgae have shown light-biomass conversion efficiencies between 1 and 4% in open systems such as ponds and even greater in closed photobioreactors (Stephens, 2010).

Light duration and intensity affect directly algal growth and microalgae photosynthesis. Microalgae needs a light/dark regime for productive photosynthesis; they, needs light for a photochemical phase to produce adenosine triphosphate (ATP), nicotinamide adenine dinucleotide phosphate-oxidase (NADPH), and also needs darkness to synthesize essential molecules for growth (Cheirsilp, 2012).

Experimental investigations reveal that the increase in light duration is directly proportional to increase in number of cultivated microalgae as well as the increase in the light intensity (Al-Qasmi, 2012).

Khoeyi Z., et. al., (2011), used three different algae samples placed in different light conditions, and found a huge difference in algal growth; the maximum biomass production was achieved when using 16:8 light/dark photoperiod duration.

When algae are incubated under blue-red light, growth rate is doubled when compared to the growth under white light (Rochet, 1986). Therefore, artificial lighting can contribute to continuous production.

b. Nutrients

The main mineral nutrients that microalgae take from environment and needs for development are the following (Malgas, 2013):

- **Carbon:** Autotrophic microalgae can use as carbon source, either the CO₂ present in the atmosphere or in exhaust gas. *Chlorella* is able to tolerate up to 400,000 ppmv of CO₂. Carbon needs can be calculated stoichiometrically knowing the composition of the biomass, resulting in a minimum of 1.85 g CO₂/g biomass. Furthermore, to ensure that microalgae will take the CO₂, the carbon dioxide partial pressure in the liquid must be 0.1-0.2 kPa.
- **Nitrogen:** is one of the essential macronutrients in the growth of microalgae. The nitrogen content of the algal biomass can be assumed from 1% to more than 10%, depending on the availability and type of nitrogen source.
- **Phosphorus:** is taken from the medium as orthophosphate (P-PO-3), whose concentration in equilibrium with the protonated forms depends on the pH of the medium. Factors such as excessively high or low pH, or absence of ions such as potassium, sodium or magnesium, makes phosphate absorption by microalgae, very slow.

- Microalgae require, other macro and micronutrients (Richmond, 2004) for their growth. Apart from C, N and P, other elements are necessary for the cultivation of microalgae, both macronutrients (S, K, Na, Fe, Mg, Ca) as micronutrients or trace elements (B, Cu, Mn, Mo, Zn, V and).

Bristol's medium is recommended for *Chlorella* by Flinn Scientific Inc., because includes all nutrients necessary.

c. pH

The pH of the medium, affect the CO₂ chemical equilibrium species, and hence the alkalinity of the medium. Each species of microalgae has a pH range in which growth is optimal, depending on which chemical species are more accustomed to assimilate. The pH in most microalgae is between 7 and 9, with an optimum between 8.2 to 8.7 (Malgas, 2013)

The photosynthetic fixation of CO₂ process causes a gradual increase in pH in the medium due to the accumulation of OH⁻. pH control is achieved by aeration or controlled injection of CO₂, but also by adding acids or bases.

Alkalinity is related to the pH of a solution, (its basicity) but measures a different property. Roughly, the alkalinity of a solution is a measure of how strong the bases are in a solution, whereas the pH measures the amount of chemical bases.

Alkalinity is the capacity of water to accept protons (acid neutralizing capacity). In natural water, main sources of alkalinity are HCO₃⁻, CO₃²⁻ and OH⁻.

Total alkalinity is defined using H₂CO₃* as PRL.

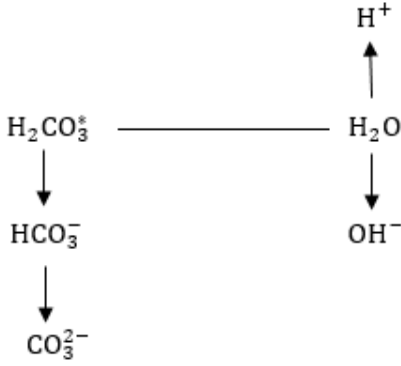


Figure 8. $H_2CO_3^*$ PRL

And the proton condition is:

$$[H^+] = [HCO_3^-] + 2[CO_3^{2-}] + [OH^-] \quad (7)$$

Where the left hand side has proton excess species, and the right-hand side has proton deficiency species.

Alkalinity is defined as net proton deficiency, therefore:

$$[Alk] = [HCO_3^-] + 2[CO_3^{2-}] + [OH^-] - [H^+] \quad (8)$$

Consequently, if a substance, component of the PRL is added, the PC does not change, i.e., adding or removing $H_2CO_3^*$ or CO_2 (aq) does not affect the total alkalinity.

At neutral pH values:



At high pH values:



d. Agitation

Agitation facilitates transport efficiency, preventing sedimentation of algae and its adhesion to the reactor walls, homogenized pH and ensures the distribution of gas and light. With proper agitation algae is subjected to rapid mixing cycles.

e. Temperature

Temperature is an important factor to consider in the growth of microalgae, since it influences the biosynthetic reaction rate coefficients (Richmond, 1986). The relationship between temperature and growth rate increases exponentially until the optimum temperature is reached.

Although a variety of microalgae are able to develop in a wide temperature range, such as the *Chlorella* species that can grow between 5 and 42°C, all exhibit a range outside of which their growth is inhibited or even die.

Kitaya Y., et. al., (2009), investigated the effects of temperature on cellular multiplication of microalgae, where the results demonstrated that the highest multiplication rate was at temperature between 27-31°C.

Effect of CO₂ on pH

Carbon dioxide is an important gas in the medium, especially because it is essential for photosynthesis of algae and aquatic plants. The dissolved CO₂, however, also affects the pH of the medium. Changes in the concentration of CO₂ will cause the pH to vary.

When carbon dioxide dissolves in the medium, largely reacts with water molecules to form carbonic acid. Carbonic acid lowers the pH of the medium. If no other factors involved, the

level of CO₂ in the atmosphere and the level of CO₂ dissolved in the medium, eventually reach an equilibrium where atmospheric CO₂ dissolves as fast as dissolved CO₂ escapes. When equilibrium is reached, the dissolved CO₂ concentration remains constant.

Equation 8 can be rewritten as:

$$[Alk] = C_{Tc} * (\alpha_1 + 2\alpha_2) + [OH^-] - [H^+] \quad (11)$$

Where C_{tc} is the total concentration of carbonic species and $\alpha_1, \alpha_2, [OH^-]$ and $[H^+]$ are pH-dependent parameters.

When CO₂ is added, alkalinity remains constant and C_{tc} decreases due to algae consumption (for photosynthesis), therefore, pH increases.

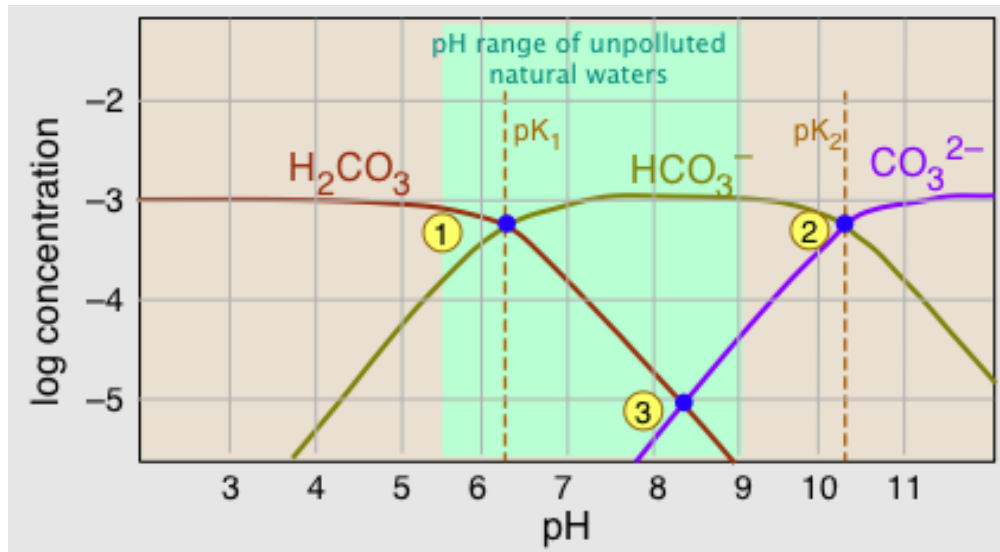


Figure 9. Log concentration diagram of a 10⁻³CO₂ solution. SOURCE: www.chem.libretexts.org

As shown in figure 9, for a pH range between 6 and 8 (pH range for algae growth), the carbonic species predominating is HCO₃⁻.

Effect of CO₂ in algal growth

Some green algae are reported to easily grow at very high CO₂ concentration. The *Chlorella* species is commonly used for carbon sequestration. It is a fresh water, single cell organism containing chlorophyll a and b, and it has a high photosynthetic efficiency to convert CO₂ to O₂ (Singh, 2014).

Chinnasamy (2009) studied the growth of *C. vulgaris* under ambient (0.036%) and elevated (20%) CO₂ partial pressures at different temperatures, and found an increase in biomass and chlorophyll concentration at 6% CO₂. No growth was obtained at ambient or elevated CO₂ levels.

Bittencourt (2009) observed that the CO₂ fixation rate of *C. vulgaris* is 251.64 mg/L/day and 86.68% biomass was produced.

Chlorella species are not limited by nitrogen or phosphorus but most likely by low dissolved organic carbon availability (Gilles, 2008). *C. vulgaris* could grow on autotrophic, mixotrophic and heterotrophic medium (Heredia, 2011).

Chlorella species showed 46% mean CO₂ fixation efficiency, at input CO₂ concentration of 10% (Ramanan, 2010).

The effect of CO₂ concentration on lipid metabolism was observed by Norihiro (2003), who found that higher unsaturation levels in low-CO₂ cells promotes the desaturation of pre-existing fatty acids, rather than up-regulation of desaturation activity.

Therefore, it has been demonstrated that CO₂ concentration plays an important role on algal growth, because there is no growth when CO₂ level are too low or extremely high, while at intermediate level CO₂ increases biomass generation and also has an important effect on lipids production.

Buffering capacity of water

The buffering capacity of water is a measure of how well it resists changes in pH.

In natural waters this buffering capacity is attributable mainly to the presence of carbonic acid species. Bases such as HCO_3^- , CO_3^{2-} , and OH^- give the water the ability to resist changes in pH when a strong acid is added. Acids like H_2CO_3 (primarily CO_2), HCO_3^- and H_3O^+ provide buffering against the addition of strong bases.

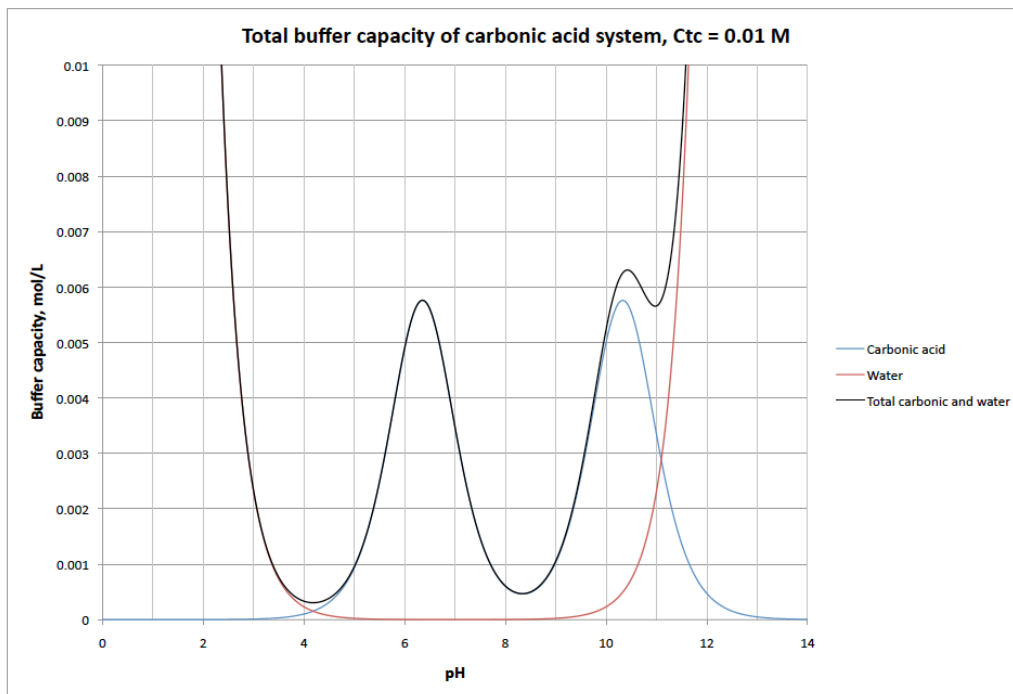


Figure 10. Buffer capacity of a natural water with total carbonic species concentration of 0.01 mol/L. SOURCE: Dr. Enrique La Motta's ENCE 6313 class notes.

Figure 10 clearly shows that in the pH range 6 - 8, buffer capacity is predominantly provided by bicarbonates.

Recuperation, fixation and transformation of CO_2 into biomass

One of the largely considered methods for CO_2 mitigation is the use of microalgae in biomass conversion in photo bioreactors (Fulke A. M., 2010). Microalgae, namely Cyanobacterial

(Cyanophyceae) and eukaryotic microalgae, green algae (Chlorophyta) and diatoms (Bacillariophyta) have been used to capture CO₂ from three different sources: atmospheric CO₂, CO₂ emission from power plants and industrial processes, and from soluble carbonate (Fulke A. C., 2013). In this context, the transfer of CO₂ from the atmosphere to the microalgae through photosynthesis is a fundamental route for CO₂ capture (Fulke A. M., 2010). In contrast, CO₂ capture from flue gas emissions from fossil fuel based power plants achieves better biomass recovery (Bilanovic, 2009). However, only a small number of algae are tolerant to the high levels of SO_x and NO_x present in flue gases. Furthermore, these gases need to be cooled down prior to injection into the growth medium. Some microalgae species can assimilate CO₂ from soluble carbonates such as Na₂CO₃ and NaHCO₃ leading to high pH of the medium because of conversion of carbonate/bicarbonate alkalinity to hydroxyl alkalinity. Such a condition tends to control invasive species since only a very small number of algae can grow in such extreme conditions (Wang, 2008).

CO₂ fixation is a process resulting from the photosynthesis produced by plants, by which carbon dioxide is absorbed and transformed into organic material or biomass.

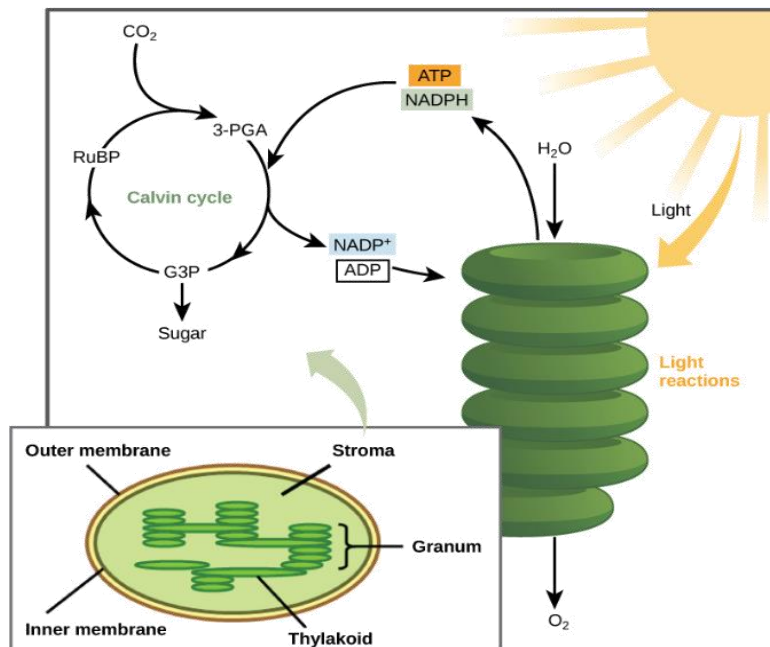


Figure 11. Light-dependent reactions harness energy from the sun to produce ATP and NADPH. SOURCE: "The Calvin cycle: Figure 1," by OpenStax College, Concepts of Biology CC BY 4.0

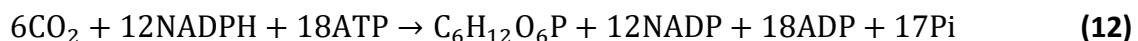
The Calvin Cycle is the most common method of carbon sequestration (Figure 11). This cycle, also known as the Calvin-Benson Cycle or "CO₂ fixation phase of photosynthesis," consists of biological and chemical processes that take place in the stroma of chloroplasts of bodies performing photosynthesis.

In photosynthesis, there is a phase known as light or photochemical, where the light energy is stored in simple and unstable organic molecules, which provide energy to make the process (ATP) and have the ability to donate electrons (reducing power) to another molecule as nicotinamide adenine dinucleotide phosphate or NADPH+H*.

As explained by Rodriguez (2009), in the Calvin cycle, carbon dioxide inorganic molecules integrate and convert into simple organic molecules from which the remaining biochemical compounds making up living beings will be formed. This process can also, therefore, referred to as carbon assimilation.

In the Calvin-Benson Cycle the first enzyme involved in fixing the CO₂ from the atmosphere by attaching it to an organic molecule, ribulose-1-5-bisphosphate, is called or known as RuBisCo (Ribulose Bisphosphate Carboxilasa-Oxygenase).

For a total of 6 molecules of CO₂ fixed, the final stoichiometry of Calvin cycle can be summarized in the equation:



Where NADPH is nicotinamide adenine dinucleotide phosphate (in its reduced form), ATP is adenosine triphosphate, NADP is nicotinamide adenine dinucleotide phosphate (in its oxidized form), ADP is adenosine diphosphate and Pi is phosphate ion.

It would represent the formation of a sugar-phosphate molecule to 6 carbon atoms (hexose) from 6 CO₂ molecules.

The Calvin-Benson cycle has three phases (Figure 12): CO₂ fixation, reduction and regeneration.

In the first phase of CO₂ fixation, "the Rubisco catalyzes the reaction between ribulose biphosphate (a pentose, is a monosaccharide 5C, RuBP) with CO₂, to create one molecule of 6 carbons, which since is unstable ends by separate into two molecules containing 3 carbon atoms each, the phosphoglycerate (PGA). The importance of Rubisco is indicated by the fact that the most abundant enzyme in nature" (Rodriguez, 2009).

In the second stage, ATP and NADPH are used to convert the 3-PGA molecules into molecules of a three-carbon sugar, glyceraldehyde-3-phosphate (G3P). This stage gets its name because NADPH donates electrons to, or reduces, a three-carbon intermediate to make G3P.

In the las stage, some G3P molecules go to make glucose, while others must be recycled to regenerate the RuBP acceptor. Regeneration requires ATP and involves a complex network of reactions (Koning, 1994).

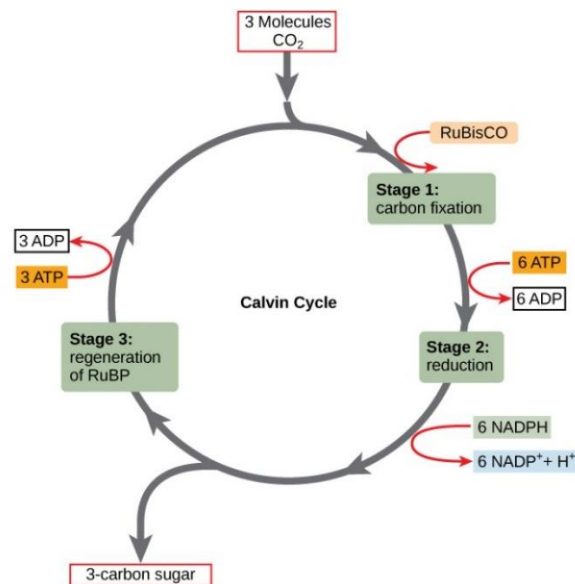


Figure 12. Calvin-Benson cycle. "The Calvin cycle: Figure 2," by OpenStax College, Concepts of Biology CC BY 4.0

In order for one G3P to exit the cycle (and go towards glucose synthesis), three CO₂ molecules must enter the cycle, providing three new atoms of fixed carbon. When three CO₂ molecules enter the cycle, six G3P molecules are made. One exits the cycle and is used to make glucose, while the other five must be recycled to regenerate three molecules of the RuBP acceptor (OpenStax, 2013).

Electroporation

Several methods based on the use of electric fields, heating, or other means to free oil from algae, without having to harvest the algae, are being developed. The premise of those methods is to supply energy to an algal culture to rupture (lyse) the cells. Lipids in the cells then spontaneously separate from the biomass, rising to the surface while the biomass sinks. The anticipated result is a solid sediment, an aqueous layer, and a free oil layer so that simple, cost-effective, and energy-efficient gravity separation recovers the oil. These systems offer the promise of substantial reduction in energy use and the elimination of solvent use (Biofuels, 2012).

a. Basics and mechanisms

Electroporation is a method of cell membrane permeabilization that is today widely used. It is an alternative method for water sterilization and food preservation (Teissie, 2002), and it is a prerequisite for cell electrofusion (Zimmermann, 1982). The phenomenon of electroporation can be described as a dramatic increase in membrane permeability caused by externally applied short and intense electric pulses.

Various theoretical models were developed to describe electroporation, among which the transient aqueous pore model is the most widely accepted. According to this model, hydrophilic pores are formed in the lipid bilayer of a cell membrane when it is exposed to external electric pulses. In the cell membrane, hydrophobic pores are formed by spontaneous thermal fluctuations of membrane lipids. In a cell exposed to an external electric field, the presence of an induced transmembrane potential provides the free energy necessary for structural

rearrangements of membrane phospholipids and thus enables hydrophilic pore formation (Neumann, 1989).

Hydrophilic pores form only in a small fraction of the membrane exposed to electric field. Even though some attempts to visualize the changes in the membrane structure caused by electric pulse application were made (Stenger, 1986), the structural reorganization and creation of hydrophilic pores has so far not been directly observed (Rols, 2006).

Cell membrane electroporation takes place because the cell membrane amplifies the applied external electric field, as its conductivity is several orders of magnitude lower than the conductivities of extra cellular medium and cell cytoplasm.

The theoretical description of the transmembrane potential induced on a spherical cell exposed to electric field is known as Schwan's equation (Neumann, 1989). The induced transmembrane potential for a spherical cell can be calculated as:

$$U_{T1} = -1.5rE\cos\varphi \quad (13)$$

Where r is the radius of the cell, E is the strength of applied electric field, and φ is the angle between the direction of the electric field and the selected point on the cell surface.

The induced transmembrane potential and therefore maximum electroporation occur at the poles of the cell exposed to the electric field facing the electrodes (Figure 13).

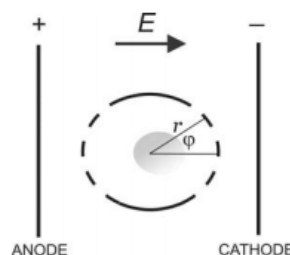


Figure 13. Cell in an electric field. (Electroporated area is presented with dashed line). SOURCE: (Kanduser, 2009)

Electroporation can be either reversible or irreversible, depending on parameters of the electric pulses. It is a threshold phenomenon: the induced transmembrane voltage imposed by external electric field should reach a critical value to trigger formation of transient aqueous pores in the cell membrane (Kinosita, 1979). The threshold membrane potential that needs to be reached in the cell membrane is between 200 mV and 1 V (Zimmermann, 1982). When the critical value is exceeded, irreversible electroporation takes place, resulting in cell membrane disintegration and loss of cell viability (Hamilton, 1967).

b. Irreversible Electroporation

Irreversible electroporation is the membrane rupture directly caused by electric pulse application (Weaver, 1996). Irreversible electroporation and Joule heating are an integral part of electrical injury, which affects especially nerve and muscle cells due to their size. Release of intracellular components from affected cells cause acute renal failure due to deposition of iron-containing molecules such as myoglobin. Successful treatment of electroporated membranes with nontoxic polymers can reduce tissue injury produced by irreversible electroporation due to sealing of electroporated cell membranes (Lee R. D., 2003). Irreversible electroporation is the desired result when it is used for microbial deactivation in water and food treatment. The applied electric pulses should cause irreversible damage of treated cells (Teissie, 2002).

For effective treatment, critical electric field parameters should be chosen properly. Typical pulse amplitude for microbial deactivation in water and liquid food is between 20 and 35 kV/cm; pulse duration, from micro-to milliseconds, and pulse number varies from ten to hundred pulses (Zhang, 1995). The main problem is the choice of optimal treatment parameters that would require minimal power consumption and would effectively disintegrate treated cells (Lebovka, 2002).

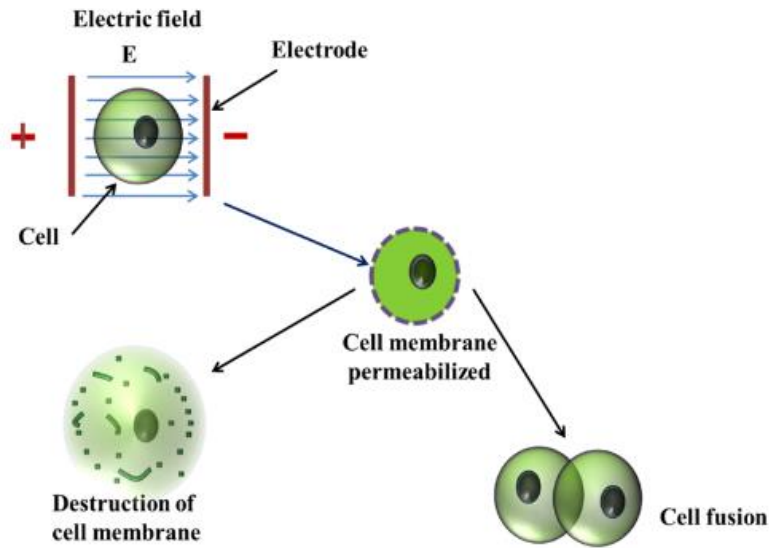


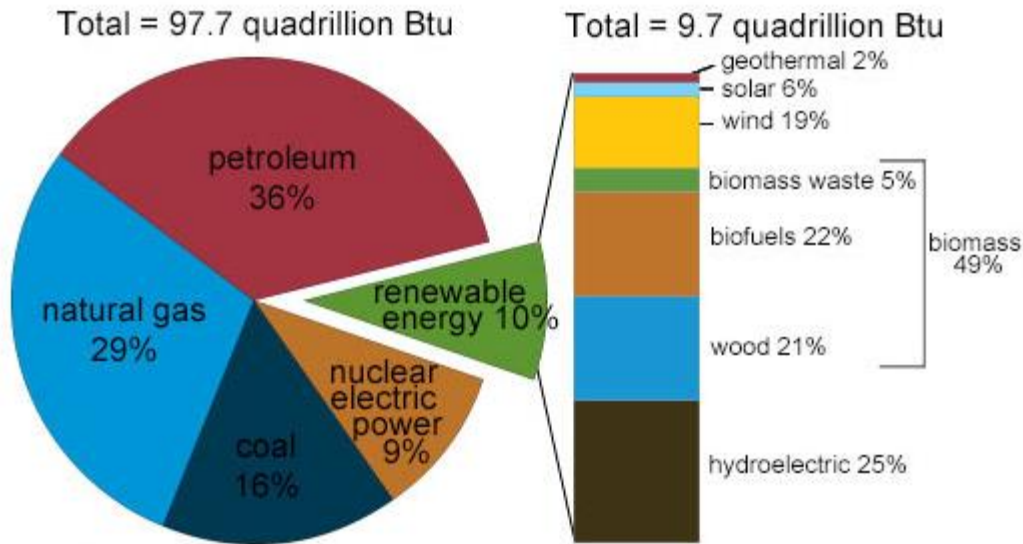
Figure 14. Irreversible electroporation. SOURCE: www.intechopen.com

Figure 14, shows that when external applied electric field reaches to the threshold values of the cell membrane, then cell membrane can permeabilized to deliver protein, small and large molecules inside the cell. When two single cells are closed to each other, then cell fusion can occur. Due to high electric field strength, which exceeds the critical value of cell membrane, irreversible electroporation can occur, resulting in cell membrane rapture (Santra, 2013).

Conversion of algal biomass to biofuel

One of the main concerns worldwide is searching for alternative or complementary sources to petroleum energy, given the forecast of depletion of existing oil sources in the planet and the problems arising from its use as greenhouse gas emissions, rising prices, and unstable markets for energy dependence on producing countries.

Biomass, within the group of renewable energy source is most commonly being used in the world: 4.8 quadrillion Btu, which is around 5% of world energy consumption (data from 2015). Figure 15, shows that petroleum, consumed the highest energy percentage (36%), followed by natural gas (29%) and coal (16%).



Note: Sum of components may not equal 100% because of independent rounding.

Figure 15. US energy consumption by energy source, 2015. SOURCE: U.S. Energy Information Administration, Monthly Energy Review, Table 1.3 and 10.1 (April 2016), preliminary data.

From the energy point of view, one of the advantages of biomass is the ability to meet all the energy needs of humanity, from transportation to the production of electricity, heat or raw materials for industry. Indeed, while most renewables only provide heat or electricity, through biomass can get a variety of gaseous solid or liquid fuels.

Current research on microalgae is mainly focused on obtaining cultures with high lipid content for biodiesel production. There are, however, in addition to such conversion, other possible energy exploitation of microalgae, similar to the use of other currently existing biomass (forest residue, urban organic waste, etc.) by thermochemical conversion, chemical or biochemical (Garcia, 2010).

Microalgae have great potential as a renewable source of biofuels, due to its rapid growth and lack of need for fertile land and fresh water for cultivation; these are two of the main disadvantages of the production of biofuels from terrestrial energy crops, such as rapeseed, palm, and others. Microalgae can double their mass several times a day and can yield more than

fifteen times the production of biofuel per hectare, which is obtained with traditional terrestrial energy crops.

Unfortunately, at present biomass production from microalgae is more expensive than with other crops. The temperature must remain between 20 and 30°C. To minimize expense, biodiesel production must rely on freely available sunlight, despite daily and seasonal variations in light levels (Kin, 2010).

A culture medium for algae must provide the inorganic elements that constitute the cells of algae. These key elements are: nitrogen, phosphorus, iron and silicon in some cases.

The biomass of microalgae contains approximately 50% carbon by dry weight. Carbon dioxide must be supplied continuously during daylight hours. Biofuel production can use some of the emissions of carbon dioxide that is released by power plants burning fossil fuels (Rodriguez, 2009).

a. Lipids

Lipids are one of the main components of the microalgae; depending on the species and growing conditions, lipids can be between 2-60% of the total dry matter as membrane components, storage products, metabolites and energy conservation (see table 1).

Triglycerides and free fatty acids (a portion of total lipid content) can be converted to biodiesel.

Table 1. Oil content of some microalgae species. SOURCE: (Malgas, 2013)

Microalgae species	Lipid content (% in dry weight)	Productivity in lipids (mg/L/day)
<i>Botryococcus braunii</i>	25.0–75.0	–
<i>Chaetoceros muelleri</i>	33.6	21.8
<i>Chaetoceros calcitrans</i>	14.6–16.4/39.8	17.6
<i>Chlorella sp.</i>	5.0–63.0	10.3–50.0
<i>Chlorococcum sp.</i>	19.3	53.7
<i>Dunaliella SP</i>	6.0–71.0	33.5 - 116.0
<i>Ellipsoidion sp.</i>	27.4	47.3
<i>Isochrysis sp.</i>	7.0–40.0	37.8
<i>Monodus subterraneus</i>	16.0	30.4
<i>Nannochloris sp.</i>	20.0–56.0	60.9–76.5
<i>Nannochloropsis sp.</i>	12.0–53.0	37.6–142.0
<i>Neochloris oleoabundans</i>	29.0–65.0	90.0–134.0
<i>Nitzschia sp.</i>	16.0–47.0	8.8–21.6
<i>Pavlova sp.</i>	30.9 – 35.5	40.2 - 49.4
<i>Phaeodactylum tricornutum</i>	18.0–57.0	44.8
<i>Porphyridium cruentum</i>	9.0–18.8/60.7	34.8
<i>Scenedesmus sp.</i>	1.9–21.1	35.1 – 53.9
<i>Skeletonema sp.</i>	13.3–51.3	17.4 - 27.3
<i>Thalassiosira pseudonana</i>	20.6	17.4
<i>Tetraselmis sp.</i>	8.5–23.0	27.0–43.3

In order to efficiently produce biodiesel from algae, the choice of strains with high growth and high oil content is recommended (FAO, 2009).

Lipid accumulation in algae usually occurs during periods of environmental stress, or what is often referred cultivation is under poor nutritional conditions. This means giving up something; rapid growth carries a low lipid content in optimal nutritional conditions, or conversely, a decrease in growth or zero growth leads to increased lipid under poor nutritional conditions (FAO, 2009). On the other hand, a peculiar result contributed by Rodolfi et al., (2009), showed an almost constant productivity and almost twice the lipid content up to 60%, after changing poor nutritional conditions in a pilot bioreactor abroad under natural light (Garcia, 2010).

b. Stages of biomass production

The production of biodiesel from microalgae is a process that consists, broadly, of the elementary stages of production of biomass rich in lipids, recovery or harvesting of biomass, lipid extraction and transesterification.

Water, nutrients, CO₂ and light, are provided to cropping systems (open, closed or hybrid) for biomass production of microalgae rich in lipids. The supplied CO₂ can come from the environment, or air, cropping systems can be coupled rich in this gas flows from industrial emissions, such as generating power plants (Garibay, 2009).

Once the microalgae biomass is produced, beginning is given to the stage of harvest, whose purpose is to remove water and concentrate the microalgal cells for further processing. This stage, greatly influences the production costs of biodiesel, so selecting a collection technique efficient and low cost is paramount. Centrifugation, sedimentation, filtration and flocculation, either individually or in combination, are the procedures most common crop, whose application depends on the properties of the kind of microalgae cultivation (particular morphologies, presence of vacuoles soda, etc.), as some have features that facilitate collection (see table 2), (Lee, 2009).

Table 2. Characteristics of Microalgae Harvesting Techniques. SOURCE: (Biofuels, 2012)

Harvest Methods	Suspended Solids Concentration (%)	Operating Costs per Gallon of Water	Cell Harvesting Efficiency	Algal Species
Centrifuging	High (< 22%)	Very high (\$20 to \$50)	> 90%	Almost all except the very fragile
Filtration/screening	Medium to high (5% to 18%)	Medium to high (\$10 to \$20)	20% to 90%	Algae with large (> 5 µm) cells
Flocculation	Low to medium (3% to 6%)	Low to medium (\$3 to \$10)	50% to 90%	Algae with low density
Bioflocculation	Low to medium (2% to 5%)	Low (\$0.20 to \$0.50)	About 90%	
Sedimentation/settling	Low (0.5% to 3%)	Low to medium (\$0.50 to \$1.50)	10% to 90%	Algae with high density

SOURCE: Adapted from Shen et al., 2009. Reprinted with permission from the American Society of Agricultural and Biological Engineers.

Once the algal biomass has been harvested, oil needs to be extracted. For processing methods that use whole cells, harvest might be all that is required for the next stage of fuel production. Biodiesel production is a technology that in most variants requires collection of the algal lipids for post processing.

Extraction of oil from biomass has proven algal to be difficult, however, it can be performed with or without breaking the cells previously. The cell disruption may be performed by conventional method, such as using the French Press that uses high pressure, or by a method most modern as is electroporation, in which an electric field is applied to cells to achieve perforation in their cell wall (Biofuels, 2012).

Oil extraction can be done with dried algae or with the wet paste from harvest. Drying is energy intensive, but yields a material that can be mechanically treated to open up access for oil extraction (Viswanathan, 2011). Once dried, oils are extracted (see figure 16 for a summary of the complete process).

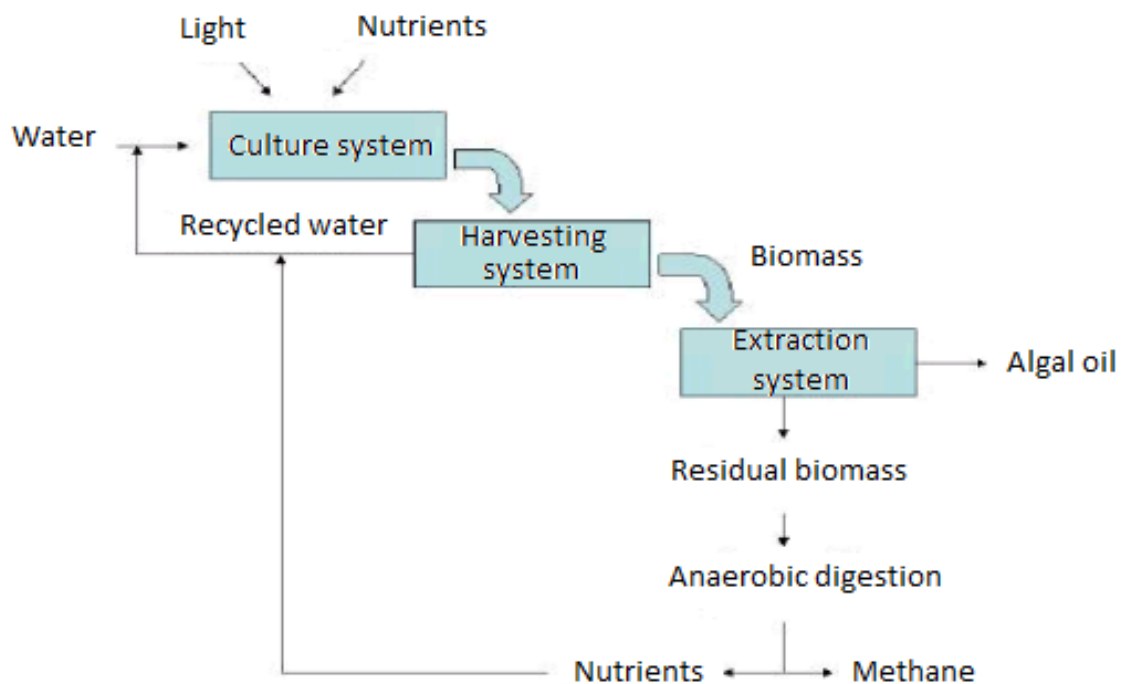


Figure 16. Process of obtaining oil from microalgae. SOURCE: (Malgas, 2013).

c. Economic Feasibility of microalgae biodiesel

The feasibility of producing biodiesel from microalgae depends on its competitiveness with fossil fuels, so that production costs are decisive. The viability estimation of this technology is possible through an analog evaluation made by Chisti, in which the maximum algae biomass production cost is estimated.

The calculation is based on the amount of biomass that provides an amount of energy equivalent to a barrel of oil (159 L). According to OPEC (OPEC Annual Report, 2008), in 2008 the average cost of a barrel of oil was US \$94.45. In order to compete with this price, spending on obtaining microalgal biomass with a lipid content of 55% (g lipids/100 g biomass) must be less than US \$323 per ton biomass (Chisti, 2008). Recently, microalgal biomass production companies have reported production costs of US \$370 per ton of biomass or lower, hence the current technology could be economically viable (Schenk, 2008). However, fluctuations in the price of oil should be considered because in the course of 2009, the cost of a barrel has significantly decreased (OPEC Basket Price, 2008), a situation that demands the reduction of production costs of microalgal biomass about one half of the value previously estimated for 2008 (US \$142 per ton of biomass) (Garibay, 2009).

The current price of WTI crude oil as of October 27, 2016 is \$49.89 per barrel, which made the production of biodiesel from microalgae unfeasible, unless the following steps are implemented:

- Select the best microalgae strains, in terms of maximum lipid content and maximum productivity.
- Establish appropriate cultivation strategies that allows maximum lipids productivity and algal biomass.
- Achieve the use of wastewater, avoiding contamination and toxic levels of concentration.

- Select the most suitable type of reactor or combination of reactors, which allow maximum biomass production at minimum cost.
- Minimize or eliminate the collection costs.
- Achieve lipid extraction and subsequent conversion to biodiesel by minimum cost strategies.

Wastewater treatment using microphytes and macrophytes

Wastewater with high concentrations of pollutants, such as nitrogen, phosphorus and heavy metals, depending on the NPDES discharge permit, must be removed before they are discharged to public water, in order to avoid problems that can lead to degradation of environmental quality. Currently, there are effective processes for removing these contaminants from wastewater, but these technological processes have a number of disadvantages of its high cost and complexity of operation, the generation of waste (sludge) or high energy consumption.

Bioremediation is one of the techniques used for the purification of waste water, in which living organisms from any realm are used. Phytodepuration is the use of green plants (macrophytes or microphyte) for purifying liquids and/or gaseous effluents.

Phytodepuration allows the simultaneous removal of pollutants from wastewater, for plants can be nutrients, and CO₂ from the atmosphere, using metabolism green plants and sun energy. As a result of metabolism, pronounced increased in biomass is produced, depending on the plant species that is used as biofilter, and existing conditions of sunlight, temperature and concentrations of nutrients in the wastewater.

As an advantage over other techniques of wastewater treatment, constructed wetlands can take advantage of the ability of green plants to metabolize pollutants with the help of solar energy. Therefore, the energy consumed for depurating is free.

Another advantage of phytodepuration is the fact that plants need atmospheric CO₂ to absorb water pollutants, setting both in its tissues biomass and releasing oxygen (O₂). Therefore, implementing a phytodepuration system not only polluted water is purified, but also helps to mitigate the greenhouse effect (Malgas, 2013).

Another type of wastewater treatment and algae production systems, are the Advanced Integrated Wastewater Pond Systems (AIWPS), which are potentially feasible for application in the developing world (Oswald W. J., 1990).

Although AIWPS may appear to be an adapted traditional pond system, each AIWPS facility is uniquely designed and incorporates a series of low-cost ponds or earthwork reactors. Depending on specific effluent characteristics, regulatory requirements, human resources, and local climatic conditions, a typical AIWPS facility consists of at least four ponds in series (Figure 17):

- An advanced facultative pond with fermentations pits.
- Algal high rate pond where photosynthetic oxygenation, oxidation, and nutrient assimilation occurs (with pedal wheel).
- Algal settling ponds.
- A maturation pond where final effluent storage and further natural disinfection occurs.

AIWPS facilities are designed to minimize the accumulation of sludge and to maximize the production of oxygen through algal photosynthesis. Algal biomass is produced and can be used as a nitrogen-rich fertilizer, or as protein-rich animal or fish feed (for further cultivation of high protein foodstuffs).

They are cost-effective, require little maintenance and have generally performed well in terms of BOD₅ and solids removal. Moreover, AIWPS require similar land area to conventional lagoons, virtually eliminate sludge disposal, produce less odor, and may be adapted to energy

(methane) recovery. However, AIWPS cost about \$15,000 to set up, and \$100 a year to power the paddle wheel and the algal settling pond needs to be desludged once to twice a year. In addition, note that this type of technology is not energy cost free.

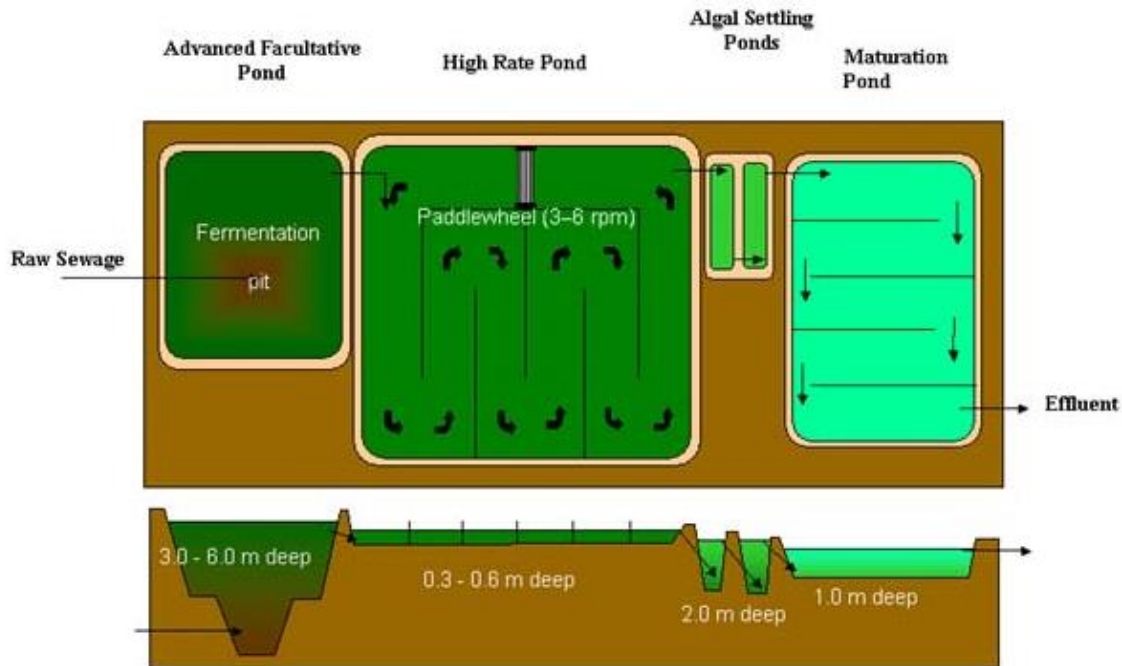


Figure 17. AIWSP system. SOURCE: www.stabilizationponds.sdsu.edu

Other studies have been made regarding the use of algae to treat wastewater, one of them is the study of Van Den Hende (2014), in which microalgal bacterial flocs in sequencing batch reactors (MaB-floc SBRs) were used to represent a novel approach to wastewater treatment. In that approach, mechanical aeration was replaced by photosynthetic aeration and MaB-floc settling separated the treated wastewater from the produced biomass. As a result, a high MaB-floc production was obtained, ranging from 0.14 to 0.26 g total suspended solids $L_{\text{reactor}}^{-1} \text{ day}^{-1}$.

A major advantage of MaB-flocs was the harvesting via a filter press with a large pore size of 200 μm , resulting in MaB-floc recoveries of 79 – 99% and cakes containing 12–21% dry matter. The results obtained may contribute to evolving MaB-floc SBRs as a valuable remediation strategy, especially for aquaculture and food-processing wastewaters.

Another study made by Dalrymple (2013), showed that microalgae feedstock production can be integrated with wastewater and industrial sources of carbon dioxide. This study analyzed algae growth on wastewater and algal production based on anaerobic digestion.

It was demonstrated that a mixed culture of wild algae species (*Scenedesmus sp. and Chlorella sp.*) could successfully be grown on wastewater nutrients and potentially scaled to commercial production.

An analysis was performed to determine the mass of algae that can be supported by the wastewater nutrients (mainly nitrogen and phosphorous) available. In that analysis, nutrients and light were assumed to be limited, while CO₂ was abundantly available. The results obtained suggested that an excess of 71 metric tons per hectare per year of algal biomass can be produced. Two energy production options were considered; liquid biofuels from feedstock with high lipid content, and biogas generation from anaerobic digestion of algae biomass. The total potential oil volume was determined to be approximately 337,500 gallons per year, and the potential biogas production was estimated to be above 415,000 kg/yr.

Current production methods for liquid biofuel production from microalgae produce approximately 60 – 70% residual biomass that is currently a byproduct. Anaerobic digestion provides biogas, but it can also provide essential nutrient recovery from lipid extracted microalgae biomass. The biogas produced from the anaerobic digestion process can be used to generate on site electrical power or thermal heat to offset biomass processing and extraction processes. When both of these processes are integrated and operated simultaneously, the benefits to microalgae biofuel production and wastewater treatment derived energy production are increased significantly (Ward, 2014). However, a pretreatment to break the algae cell wall has to be done in order get a high production of biogas and therefore of energy (Golueke, 1956).

Chapter III

Laboratory Equipment and Experimental Set-up

Laboratory equipment

a. Shaking water bath

The water bath used in this research was purchased from General Laboratory Supply, Inc. of Pasadena, Texas. This equipment has a capacity of 18 liters and includes a universal tray to hold up to 4, 1000 ml flasks and a polycarbonate lid that limits evaporation and conserves energy (Figure 18).

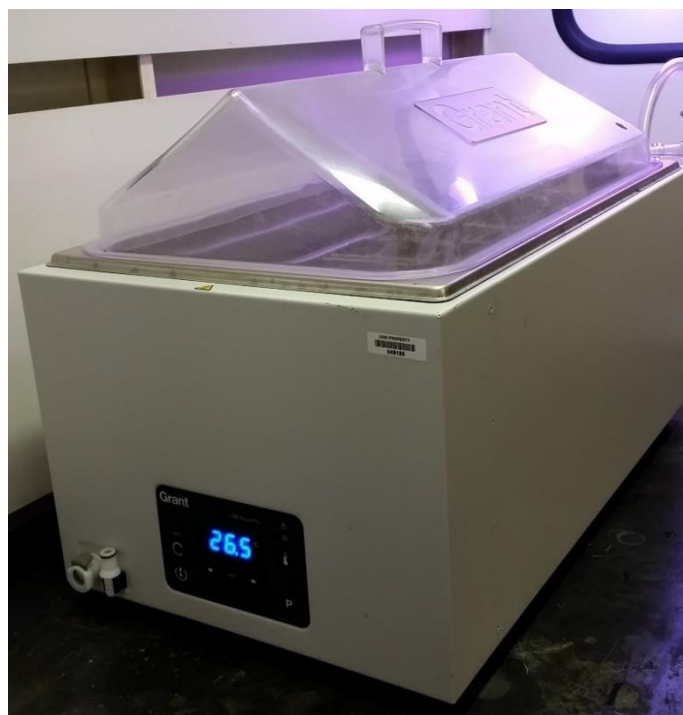


Figure 18. Shaking water bath.

The dimensions of the water bath are 420 x 235 mm, the temperature range is ambient +5 to 99°C and the linear shaking speed range from 20 to 200 rpm (depending on load). Thus, it is possible to change the temperature and the shaking speed.

For the first part of the research, two types of 1-L flask and 1-L bottle were used. (Figure 19a) For the second part, a 5-gallon bottle was used. (Figure 19b) Each flask and bottle had a 3-hole rubber stopper for the connections between them, the air supply and the CO₂.



Figure 19. Flasks used in the experiments. (a) Experiment 1, (b) Experiment 2.

The flasks and bottles were placed inside the tray (Figure 20) to stand firm and keep constant temperature.

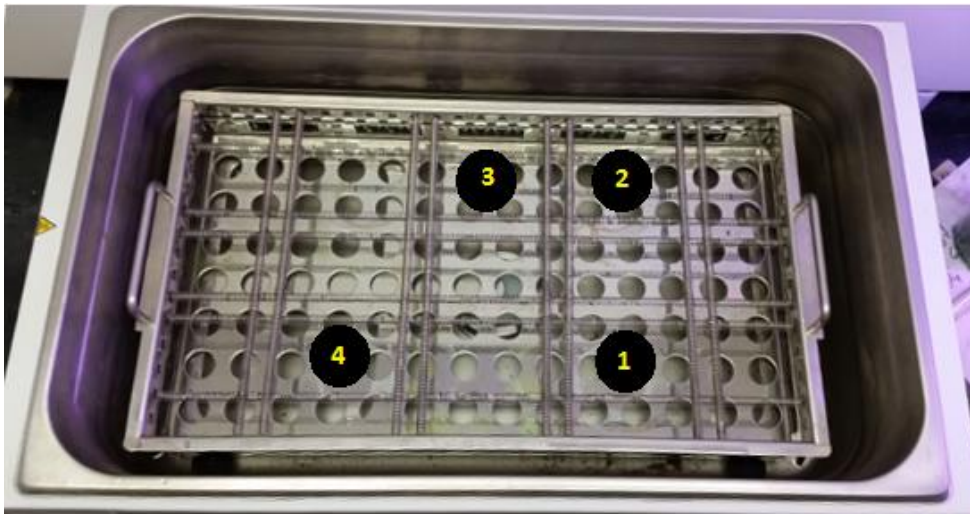


Figure 20. Flask arrangement (first part).

b. Electrochemical batch reactor

The reactor used in this research was purchased from Ecolotron Inc. of Seabrook, TX. Its design is property of Gavrel et al. under US Patent No.: 7087176 B2, registered on August 8th, 2006. This unit includes a plate and frame design and can be tightly closed mechanically. The spacer plates, which are sealed and non-electrical, completely enclose and isolate all fluids, electrical contacts and electrodes within the reactor structure. This reactor design has the advantage of being versatile enough to allow for modifications of its original configuration. Thus, it is possible to vary the number of cells, electrode material, dimensions and even the positioning of the plates using the same frame (Rincon, 2013).



Figure 21. Electrochemical batch reactor.

For this research, spacer plates with insulator seal on both sides and titanium electrodes coated with iridium oxide were used. Dimensions are shown in Figure 22.

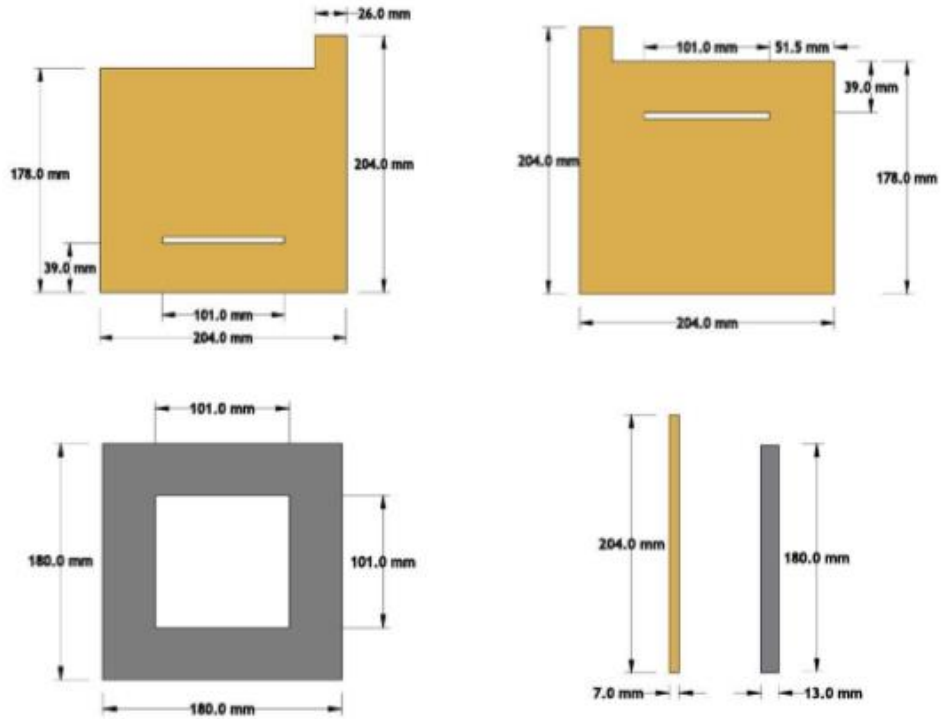


Figure 22. Electrode and spacer dimensions. SOURCE: (Rincon, 2013).

The electrodes were placed inside the reactor horizontally, parallel and with their openings opposite to each other as shown in figure 23.

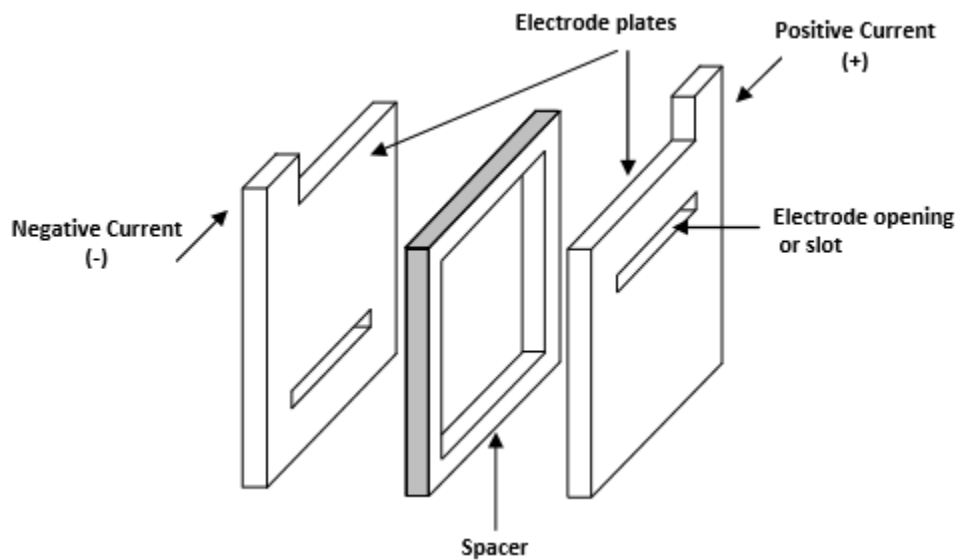


Figure 23. Cell arrangement. SOURCE: (Rincon, 2013).

The reactor was modified by Luis De Grau in (2015), so all the gases (oxygen and hydrogen) could freely escape. The modification consisted in perforating a hole in one of the spacer plates (Figure 24). Before this modification, gases accumulated inside the reactor, occupying a significant volume, therefore reducing the amount of sample being treated and causing the flow that exited the reactor to be variable. With this modification, this problem was solved.



Figure 24. Opening for gas exit. SOURCE: (De Grau, 2015)

Laboratory methods

A detailed explanation of each of the following methods is presented in Appendix A.

a. Medium preparation for algae growth

10 ml of Bristol's medium were added to the beaker and then was filled with deionized water until 1-L mark. After that, 2 pinches of soil, 20 mg of Calcium Carbonate and 250 mg of Sodium Bicarbonate were added and mixed until homogeneous mix was achieved (see appendix A for details).

b. pH

pH was measured using Thermo Scientific Orion Star Plus Meter and Thermo Orion pH meter.

Each pH meter was calibrated (using 4, 7 and 10 Acros buffer solutions), rinsed with deionized water, dried and placed into a well-mixed sample to take measurements (see appendix A for details).

c. Conductivity

Conductivity was measured using Thermo Scientific Orion Star Plus Meter.

Orion Star Plus meter was calibrated (using 3163 and 3161 YSI calibrator solutions), rinsed with deionized water, dried and placed into a well-mixed sample to take measurements (see appendix A for details).

d. Alkalinity

Alkalinity was measured by titrating the sample with sulfuric acid following HACH method 8221 (see appendix A for details).

e. Calcium

Calcium was measured by titrating the sample with EDTA following HACH method 8222 (see appendix A for details).

f. Turbidity

Turbidity was measured using HF Scientific Micro 100 turbidimeter.

Turbidimeter was calibrated (using 1000, 10 and 0.2 NTU calibration solutions). Each sample was poured into a clean cuvette three times to rinse it. After this, the cuvette was filled with the sample, covered with a cap and dried, then was placed in the optical well and indexed to the lowest reading (see appendix A for details).

g. Chlorophyll A

Chlorophyll A was measured using Eppendorf centrifuge 5810 R and DR 5000 HACH spectrophotometer, following the Wegmann-Metzner method using 90% acetone (see appendix A for details).

h. Cell wall break

For cell wall break experiment, Ecolotron reactor, BK Precision High Current DC Regulated Power Supply (Model 1791), OMANO OMFL400 Fluorescence Compound Microscope, Jenoptik ProgRes CapturePro 2.5 Camera and titanium electrodes coated with iridium oxide, were used. Spacers and electrodes were placed in such a way that the reactor had one cell with a volume of 285 ml.

The power supply was connected to each electrode and the experiment was performed by applying constant voltage and constant current to achieve algae cell wall annihilation (see appendix A for details).

Experiment design

The experimental phase of this research was conducted at The University of New Orleans, in the Center for Energy Resource Management (CERM), New Orleans, Louisiana. The algae used in this research was *Chlorella Vulgaris* Size 100, which was purchased from Flinn Scientific, Inc.



Figure 25. *Chlorella Vulgaris* culture.

The algae (Figure 25) were cultured in Bristol's medium, whose concentration in g/L is: Calcium chloride, $\text{CaCl}_2 \cdot 2\text{H}_2\text{O}$, 1 g, Sodium chloride, NaCl , 1 g, Magnesium sulfate, $\text{MgSO}_4 \cdot 7\text{H}_2\text{O}$, 3 g, Sodium nitrate, NaNO_3 , 10 g, Potassium phosphate, monobasic, KH_2PO_4 , 3 g, Potassium phosphate, dibasic, K_2HPO_4 , 3 g, and other solutions as: Pringsheim's soil-water, 40 mL, Iron(III) chloride solution, 1%, < 1 mL. However, since the medium was corrosive for the algae to grow, 20 mg/L of Calcium carbonate and 250 mg/L of Sodium bicarbonate were added to get an alkalinity around 200 mg/L as CaCO_3 . This amount of chemicals needed were calculated using RTW4 (With corrected Ks, modified 7-21-16) spreadsheet.

a. Experiment 1: Algae cultivation under a range of CO_2 concentrations from 0 to 20%.

10 ml of algae were taken from the culture using Pasteur pipets into a 1-L flasks (and bottles) containing 500 ml of Bristol's medium. Flasks were fitted with 3-hole rubber stoppers for

connecting the air supply, the different percentages of CO₂ (0, 5, 10, 15, 20) and interconnect with the other flasks to prevent evaporation and ensure the same air flow was supplied to each flask. Cultures were grown on the water bath at temperatures of 25 ± 1°C with an illumination period of 16:8 (Light/Dark) using Hgrope 5W Blue-Red Light LED Grow Plant Lamp. The agitation provided by the bubbles to the culture ensures continuous mixing that under normal conditions prevents settling of the culture suspension to the flask bottom and cell adherence to the flask walls.

The air flow supplied was 10 L/min, from that, each CO₂ percentage and flow rate was as follows:

Table 3. CO₂ percentage and flow rate.

Flaks number	Air		CO ₂ %	CO ₂	
	(L/min)	(L/sec)		(L/min)	(L/sec)
0	10	0.17	0	0	0
1	10	0.17	5	0.5	0.0083
2	10	0.17	10	1.0	0.017
3	10	0.17	15	1.5	0.025
4	10	0.17	20	2.0	0.033

It is important to highlight, that since the percentage of CO₂ in the air is 0.002%, it was neglected in the calculations.

The CO₂ and air flow rate, were measured every day using OMEGA 5 L/min and 25 L/min air flow rotameters, to ensure that the correct flow was going to each flask. Since the rotameters were only for air flow, the following formula was used to correct the lecture for CO₂ measurements:

$$SCFM_{CO_2} = \frac{SCFM_{Air}}{\sqrt{\frac{SG * T_o * 14.7}{1.0 * 530 * P_o}}} \quad (14)$$

Where:

SG = Specific gravity CO₂ = 1.5189

To = Temperature at operating conditions, Rankine = 527.67°R

Po = Pressure at operating conditions, psia = 14.7 psia

Therefore, the following readings (table 4) were used for each flask to get the desired CO₂ flow rate:

Table 4. Readings using air flow rotameter to get desired CO₂ flow rate.

CO ₂ %	Air reading		CO ₂	
	(L/min)	(L/sec)	(L/min)	(L/sec)
0	0	0	0	0
5	0.6	0.01	0.5	0.0083
10	1.2	0.02	1.0	0.017
15	1.8	0.03	1.5	0.025
20	2.4	0.04	2.0	0.033

In this experiment, temperature, conductivity, pH and turbidity, were measured daily during 40 days. The main objective of this first experiment was to determine the maximum CO₂ concentration that can be added to an algal suspension (within the emission range from industrial plants) and the optimum pH and alkalinity to maximize algal biomass.



Figure 26. Experiment 1 set up, showing the connections between the flasks, air supply and CO₂ cylinder.

b. Experiment 2: Growth of a large volume of algae using the optimum CO₂ concentration found in experiment 1 (15%).

Once the optimum operating conditions were defined (temperature of 25°C, light/dark period of 16:8 hours, air flow rate of 10 L/min and 15% CO₂), the culture that showed better growth was poured into a 19 L (5-gallon) bottle containing 10 L of Bristol's medium (Figure 27). The same procedure as in experiment 1 was followed for four weeks, to get a large amount of culture in preparation for the electroporation treatment.

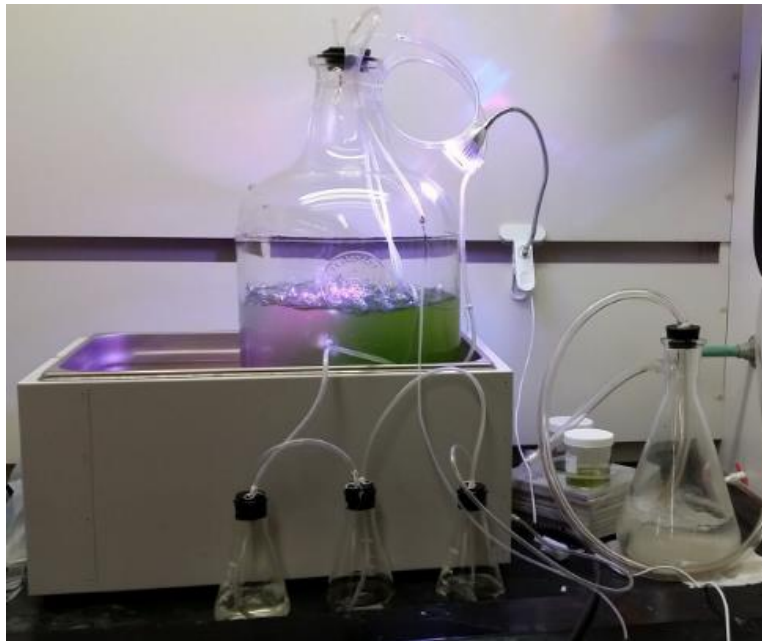


Figure 27. Experiment 2 set up, showing the bottle inside the water bath and the flasks interconnected to prevent evaporation.

Algae growth was determined by measuring turbidity values every day.

To prevent evaporation in both experiments, a 2-L flask and 3, 250 ml flasks filled with water were connected in between the air supply and the reactors.

c. Experiment 3: Irreversible electroporation of algae cell wall.

Once a significant amount of algae was produced, the electroporation experiment began. For that, samples from the 15% flask were taken using pipettes and poured into the reactor using a funnel. Effluent was collected in a tray placed under the reactor after releasing the hydraulic jack.

Inside the reactor a total of two electrodes and two spacers were used. The electrodes were connected with DC current to BK Precision High Current DC Regulated Power Supply, Model 1791. Once the electric charge was applied to the electrodes, the entire volume had to be discarded after sampling. Consequently, the reactor volume (285 ml) was small in order to save algal culture. Figure 28 shows that the reactor had one cell.



Figure 28. One cell batch reactor.

Chapter IV

Results and Data Analysis

The algae culture was grown for six weeks. Temperature, pH, conductivity and turbidity were measured every day and alkalinity and calcium were measured at the beginning and end of the experiment. Three experiments are presented in this chapter: in experiment 1, algae suspension was grown under established parameters of temperature, light period, alkalinity, air flow rate and different CO₂ concentrations; in experiment 2, once the optimal growth parameters were defined, a large algae volume was grown; and finally, in experiment 3, electroporation treatment using an EC batch reactor connected to DC current was done in order to break the cell membrane and determine the effective parameters to achieve a complete breaking.

Experiment 1

a. Turbidity

The information presented in Table 5 corresponds to the turbidity (main factor in determining the rate of growth of algae) for each CO₂ percentage.

Table 5. Turbidity results.

Days	Turbidity				
	Flask 0 (0% CO ₂)	Flask 1 (5% CO ₂)	Flask 2 (10% CO ₂)	Flask 3 (15% CO ₂)	Flask 4 (20% CO ₂)
0	5.4	-	-	-	-
1	3.11	-	-	-	-
2	5.22	3.19	3.87	3.58	3.94
3	6.09	2.61	3.36	4.4	4.49
4	8.57	6.02	6.05	6.49	6.5
5	11.5	5.61	4.64	10.2	6.98
6	15.6	15.4	5.05	12.8	8.55
7	22.4	8.29	5.75	17.3	13.4
8	27.4	7.15	7.13	23.3	29.4

(Table 5 continued)

Days	Flask 0 (0% CO ₂)	Flask 1 (5% CO ₂)	Flask 2 (10% CO ₂)	Flask 3 (15% CO ₂)	Flask 4 (20% CO ₂)
9	46.4	10.4	8.6	27.1	46.1
10	41.6	11.5	8.75	29.6	23.3
11	39	16.9	13.9	70.7	80.6
12	33.2	22	19.2	70.8	64.6
13	26.8	36.9	35	75.2	83
14	34.7	37.7	44.5	82.2	48.6
15	12.1	94	48.2	91.9	66.4
16	20.7	40	39.4	92.3	82.2
17	12.6	50.3	37.3	103	73.3
18	11.7	62.5	43.8	125	92
19	19.4	51.1	46	119	96.1
20	10.1	58.7	56.7	118	69.1
21	6.79	53.7	44.8	148	81.7
22	14.2	46.7	35.4	174	90.2
23	17.1	54.2	43.5	199	106
24	11.1	55.8	41.1	192	131
25	8.85	67.8	37.6	220	124
26	6.83	49.1	36.5	219	164
27	13.9	52.1	36.1	215	176
28	15.1	61.6	46.8	294	233
29	12.8	83.6	57.4	294	291
30	18	33.2	30.1	224	164
31	-	69.1	38.4	258	256
32	-	75.6	49.5	304	251
33	-	80.9	36.5	319	128
34	-	57.8	45.3	241	262
35	-	85.1	52	282	362
36	-	83	38.9	241	236
37	-	97.1	45.3	260	273
38	-	128	57.5	305	320
39	-	95.3	44.3	186	343
40	-	125	52	195	279

(NOTE: 0% CO₂ experiment was stopped at 30 days because algae were not growing).

Total suspended solids (TSS) are particles that are larger than 2 microns. Most suspended solids are made up of inorganic materials, though bacteria and algae also contribute to the total solids concentration (Kentucky Water Watch).

Turbidity measurements are often used to estimate total suspended solids. The turbidity is based on the amount of light scattered by particles in the water column. The more particles that are present, the more light that will be scattered (Perlman, 2014).

When turbidity is low, more light can penetrate through the water column. This creates optimal conditions for algal growth. In return, growing algae create a turbid environment (CEES, n.d.).

Therefore, as algae are growing turbidity increases. Consequently, as shown in Table 5, turbidity in flask 3 increased with time, indicating progressive algae culture growth.

Also, to determine the maximum CO₂ concentration that can be added to the algal suspension within the emission range from thermoelectric plants, a non-linear regression analysis to build the logistic growth curve for each CO₂ percentage was made, using turbidity values and equations 3 to 6.

The following results were obtained:

- **Flask 0 (0% CO₂)**

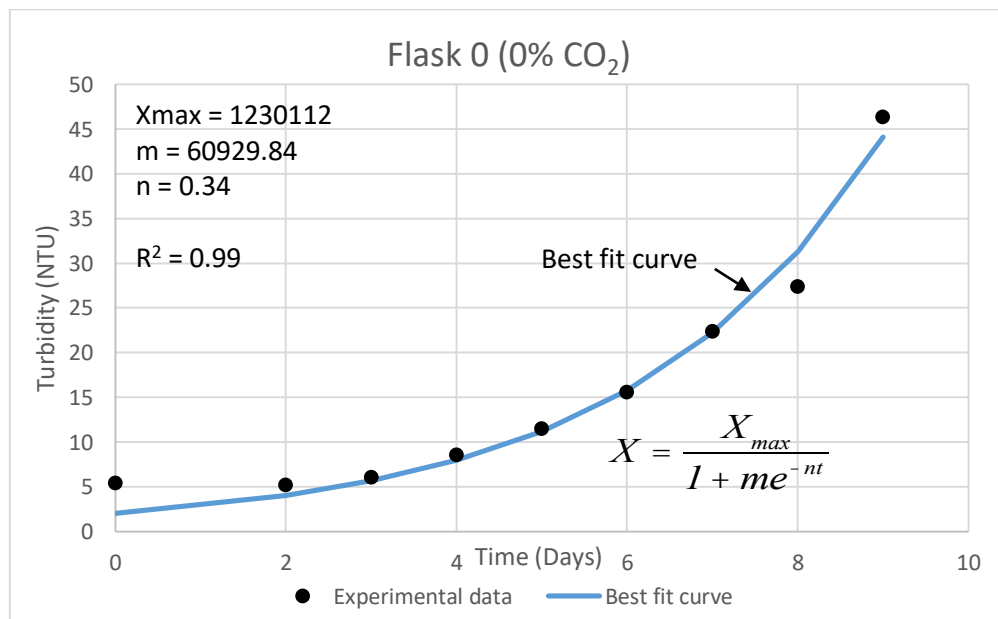


Figure 29. Non-linear regression plot for flask 0.

Although the experiment lasted 40 days, only the first 9 days were taken into account for the analysis, because a perfect fit to exponential growth curve was observed during this period. However, this gradual increase in turbidity was due to the presence of soil from the culture medium and not from algae growth. As shown in Figure 29, no growth was observed during the experiment, the sample color remained the same from start to end.

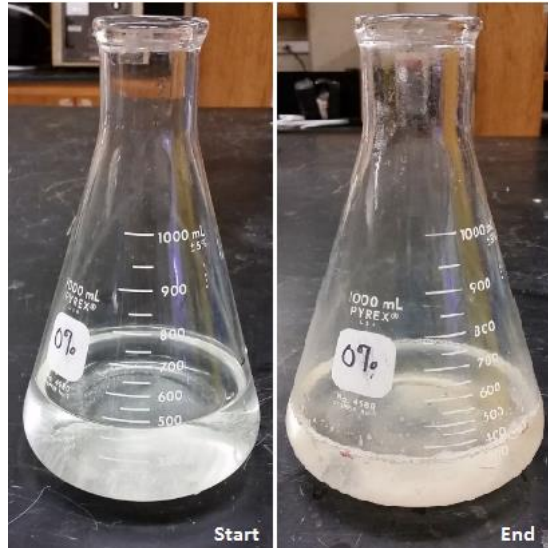


Figure 30. Algae growth from start to end for flask 0.

- **Flask 1 (5% CO₂)**

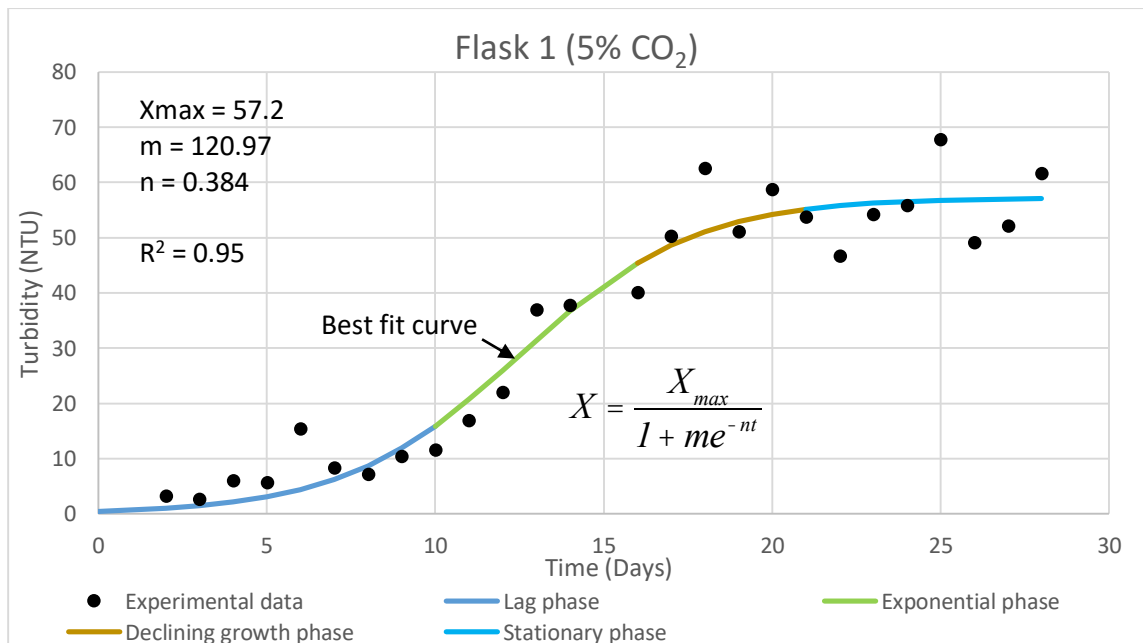


Figure 31. Non-linear regression plot for flask 1.

As shown in Figure 31, for 5% CO₂, the values obtained led to a perfect fit to s-shaped logistic growth curve using the same model. However, it is noted that the culture reached stationary phase, i.e., the maximum concentration possible was obtained at a very low value of 57.2 µg/L, even though the rate of growth was moderately slow.



Figure 32. Algae growth from start to end for flask 1.

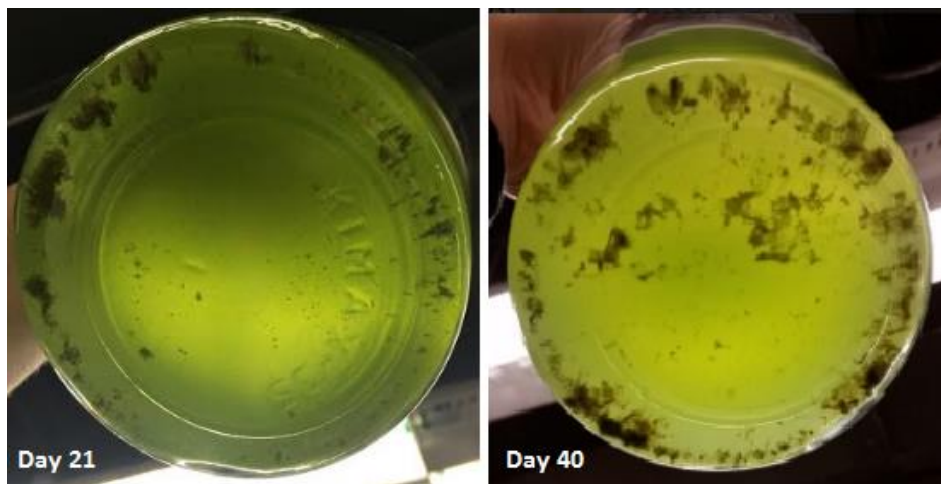


Figure 33. Clumps in the bottom of flask 1 for days 21 and 40.

Figure 32 shows the change in color (due to chlorophyll and algae concentration) from start to end of flask 1. Figure 33, shows that for days 21 and 40, a lot of clumps were observed at the bottom of flask 1, which perfectly adapts to the beginning and end of the stationary phase because algae death is increasing during this time.

- **Flask 2 (10% CO₂)**

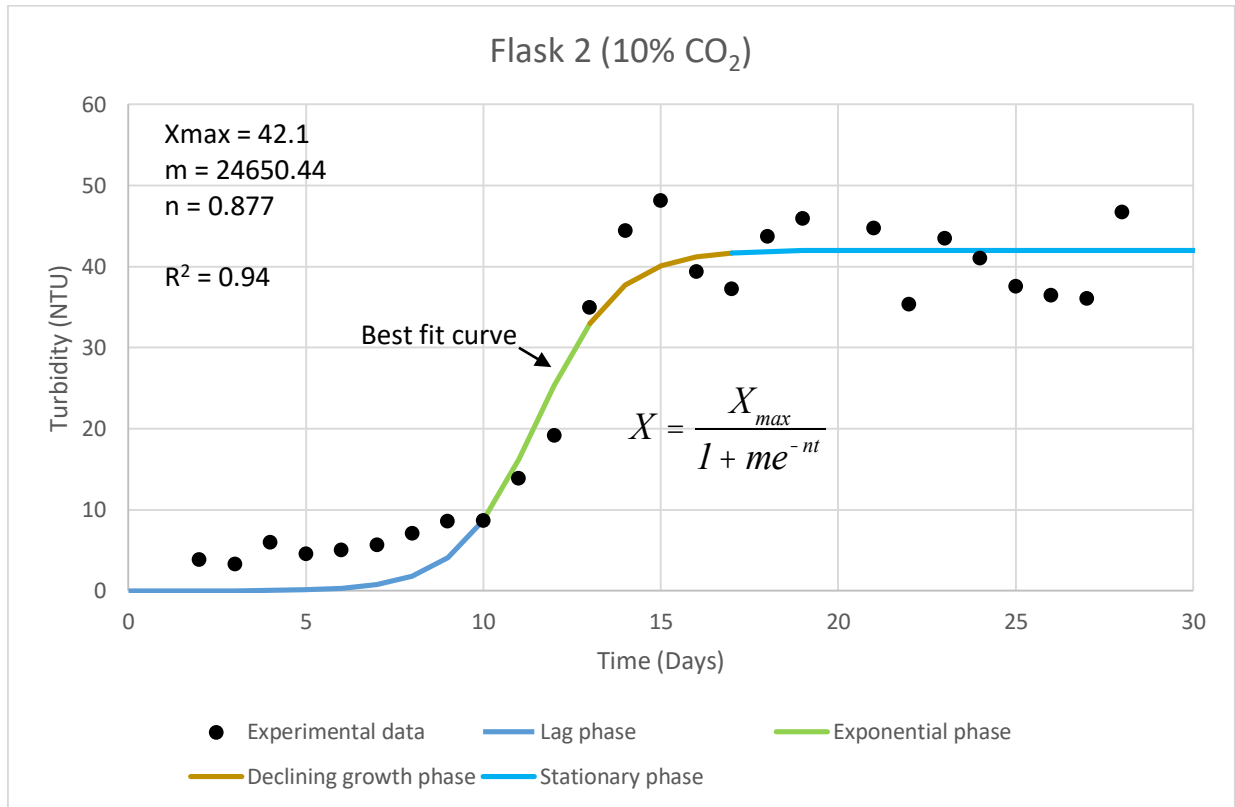


Figure 34. Non-linear regression plot for flask 2.

The logistic growth curve for flask 2 shows a prolonged stationary phase at very low X_{max} (42.1 µg/L) and a very short exponential phase (about 3 days). This indicates that the algae were not adapted properly to the medium, which prevented proper growth. It is important to highlight that the rate of growth was extremely high, although the maximum concentration was the lowest of all CO₂ percentages studied.



Figure 35. Algae growth from start to end for flask 2.

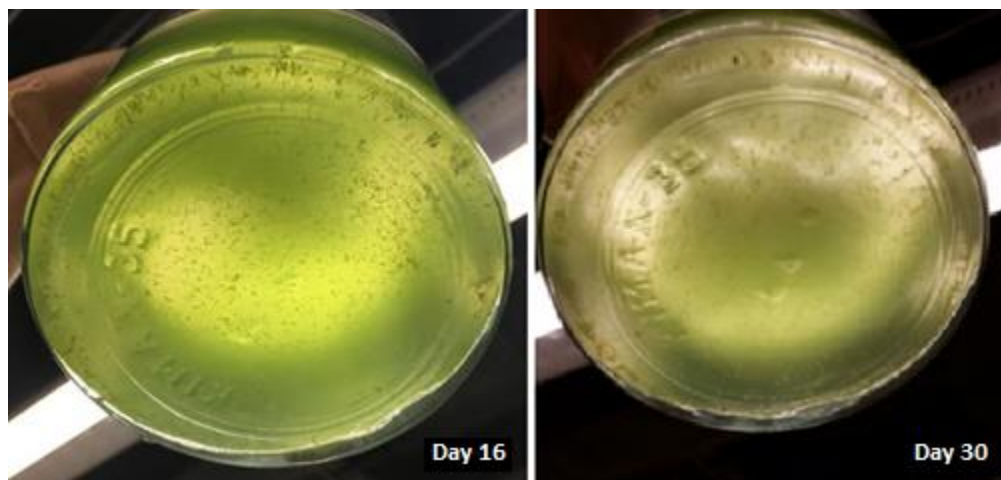


Figure 36. Clumps in the bottom of flask 2 for days 16 and 30.

Figure 35 shows the change in color, due to chlorophyll and algae concentration, from start to end of flask 2. Figure 36, shows that for days 16 and 30, a low amount of clumps was observed at the bottom of flask 2, which adapts to the beginning and end of the stationary phase. The change in color is due to the lack of chlorophyll, due to algae death.

The light green color present in flasks 1 and 2, was due to low algae growth, therefore, low chlorophyll concentration. However, based on the results obtained, adding 5% CO₂ leads to better final concentration results than adding 10% CO₂.

- **Flask 3 (15% CO₂)**

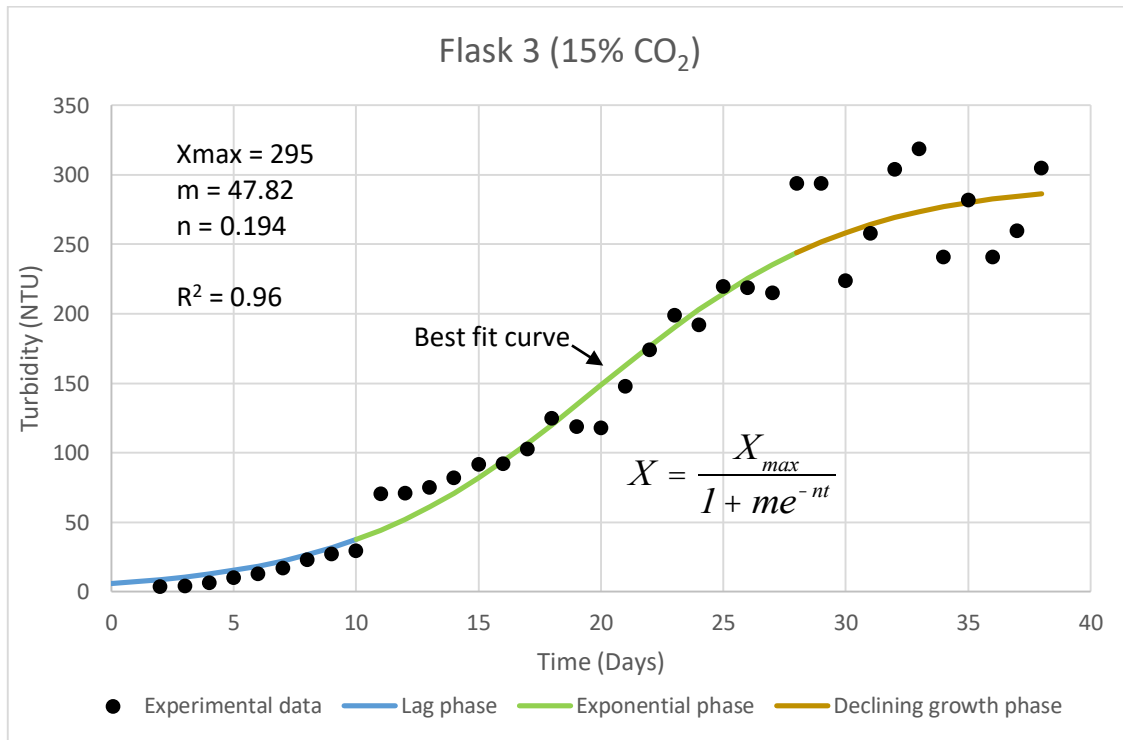


Figure 37. Non-linear regression plot for flask 3.

Figure 37, shows a fairly close fit in the first phase of growth, this means that algae adapted perfectly to the medium and grow gradually as time passes. The exponential phase in this sample had a duration of approximately 18 days, in which a significant increase in algal biomass was observed.

Although the X_{max} value under this CO₂ percentage was high (295 µg/L) and its rate of growth was slow, it is observed that the curve was starting to reach its stationary phase, that is, under present conditions of the medium volume, no significant growth will be observed.

As shown in figure 38, an important difference from start to end was observed in flask 3, since it reached a dark green color, which represents high chlorophyll concentration.

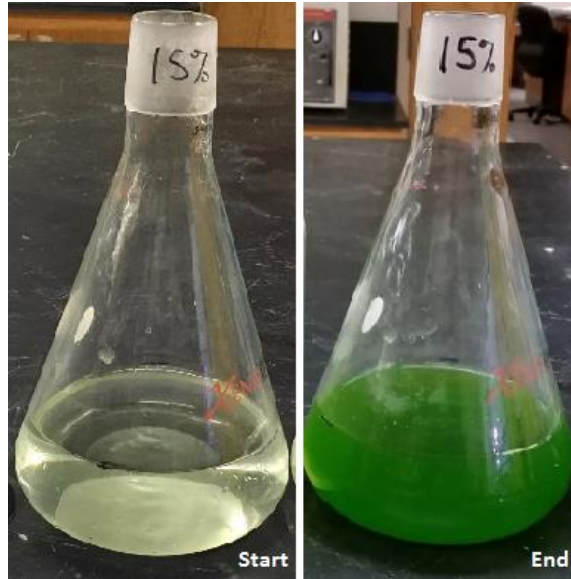


Figure 38. Algae growth from start to end for flask 3.

- **Flask 4 (20% CO₂)**

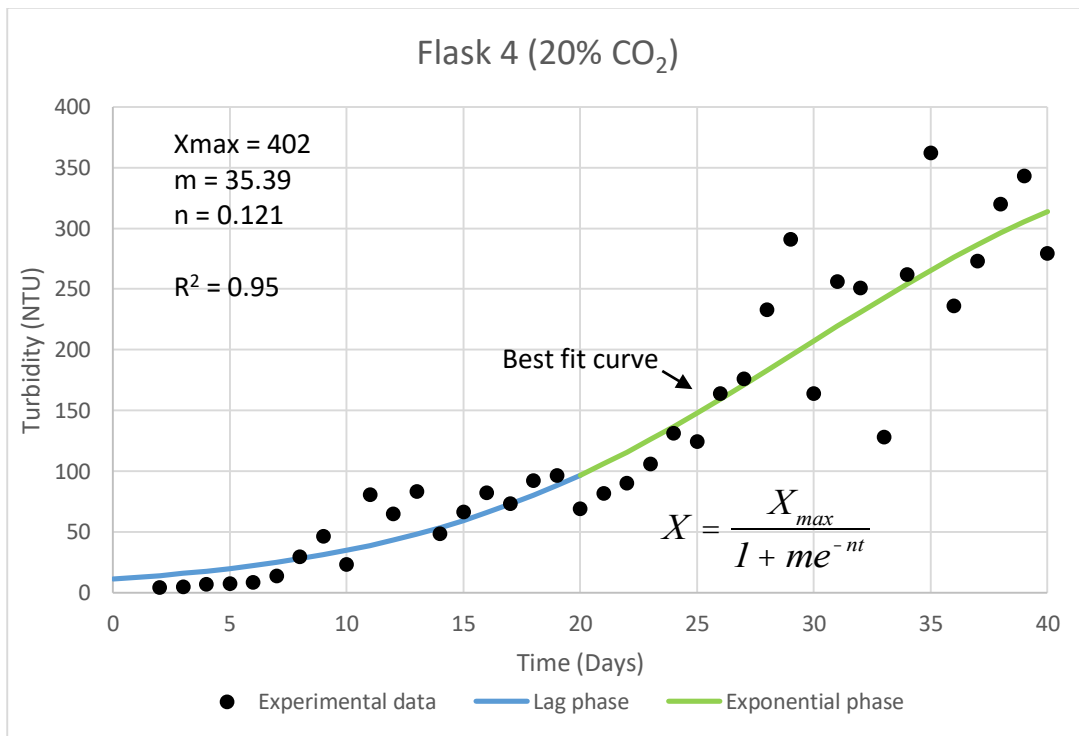


Figure 39. Non-linear regression plot for flask 4.

As shown in figure 39, only two phases of growth can be observed, lag and exponential phase. In the first phase, a duration of approximately 20 days was observed, indicating that it was

difficult for the algae to adapt to the environment under this CO₂ concentration; and in the second phase, it is observed that although it took more time and had the highest X_{max} (402 µg/L), algae could continue to grow, as the stationary phase had not been yet reached at the end of this experiment.

Figure 40 shows the change in color from beginning to end of flask 4, due to increasing chlorophyll and algae concentration.

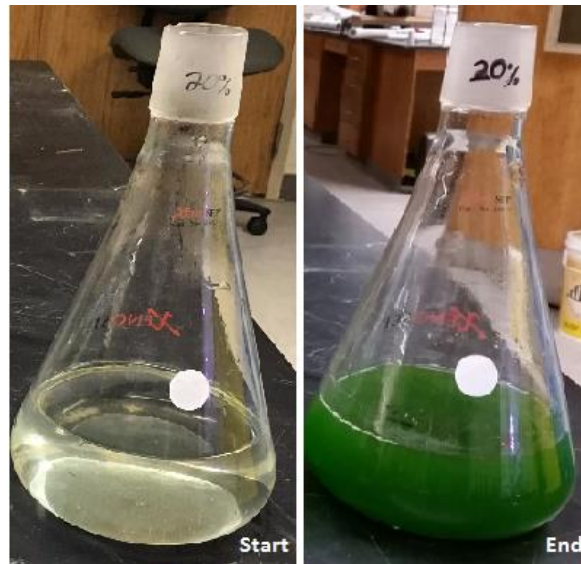


Figure 40. Algae growth from start to end for flask 4.

Consequently, from Figures 29 to 40, it can be noted that, for 0% CO₂, there was not growth; for 5 and 10% CO₂, the maximum concentration was reached very fast; for 15% the algae concentration increased at a high paced and for 20% CO₂ both adaptation and growth takes longer. Therefore, the maximum CO₂ concentration that can be added to a *Chlorella vulgaris* suspension, based on the emission range from thermoelectric plants, was 20%.

b. pH

In order to determine the pH of the culture, an average of the activity of the hydrogen ion was calculated using the pH values of flask 3 (culture that showed better growth) and equation 15.

$$\{H^+\} = 10^{-pH} \quad (15)$$

Once the average was calculated, the pH was obtained using equation 16.

$$pH = \log \frac{1}{\{H^+_{Avg}\}} \quad (16)$$

The pH of flask 3 was 6.64.

c. Alkalinity measurements

The alkalinity of wastewater at Marrero, LA, wastewater treatment plant, is between 100 to 200 mg/L CaCO₃ (De Grau, 2015). Since the initial alkalinity of the algal growth medium was 10 mg/L CaCO₃, it was necessary to add of 20 mg/L of calcium carbonate and 250 mg/L sodium bicarbonate, in order to increase alkalinity and to provide sufficient buffering capacity.

The amounts of chemicals to be added were calculated using the spreadsheet RTW4, using the following measured initial values:

- TDS, mg/L = 403.84
- Temperature, °C = 18.2
- pH = 6.3
- Alk, mg/L CaCO₃ = 10
- Ca, mg/L CaCO₃ = 6

The results obtained after the addition of chemicals were:

- Alk, mg/L CaCO₃ = 180
- Precipitation potential, mg/L = -0.63
- Langelier index = -0.03

Alkalinity was measured at the end of experiment 1. Results of titration with sulfuric acid and EDTA are:

Table 6. Alkalinity results.

%CO₂	Volume spent (Sulfuric acid)	Volume spent (EDTA)	Alk (mg/L CaCO₃)
5	25.9	4.3	647.5
10	12.6	2.5	315
15	24.7	2.5	617.5
20	38	5.1	950

As shown in table 6, alkalinity increased significantly for each CO₂ percentage. Therefore, in order to determine what was the factor that produced this change, an alkalinity test to the medium was performed at different stages of preparation, obtaining the following results:

Table 7. Alkalinity trial.

Type of medium	No soil or chemicals	No soil with chemicals	With soil and chemicals
Alk (mg/L CaCO₃)	13.3	130	163.3

From table 7, it can be seen that, as stated before, the addition of calcium carbonate and sodium bicarbonate significantly increased alkalinity, however, the small amounts of soil added, as recommended by Flinn Scientific Inc., also increased alkalinity. This is because these chemicals and the soil components, are not part of the proton reference level, and consequently, they produce a change in the total alkalinity.

Such a large increase is because the medium was replaced constantly throughout the experiment, to ensure that it was kept fresh and that algae never had to compete for resources (Wood, 2005).

d. Chlorophyll A measurements

Using the Wegmann-Metzner method for chlorophyll determination (Eq. 17), a volume of culture of 0.005 L and a light path length of 1 cm, the following results were obtained:

Table 8. Chlorophyll concentration.

%CO ₂	λ663	λ644	λ750	Volume of extract (ml)	Relative concentration of Chlorophyll A	Pigment concentration per volume of culture (µg/L = mg/m ³)
5	0.177	0.058	0.002	3	1.751092	1050.6552
10	0.223	0.14	0.071	3	1.502258	901.3548
15	1.015	0.427	0.085	3	9.265044	5559.0264
20	0.863	0.303	0.003	3	8.5826	5149.56

As shown in table 8, flask 3 had the highest chlorophyll concentration at the end of the experiment, 5559.03 µg/L, which explains the dark green color obtained at the end of the experiment. This value adapts to the conclusion made by Chinnasamy in 2009, which state: “An increment in CO₂ levels greater than 6% decreases the concentration of chlorophyll and biomass to less than 11 and 210 µg/ml, respectively”.

e. Correlation between turbidity and chlorophyll a concentration

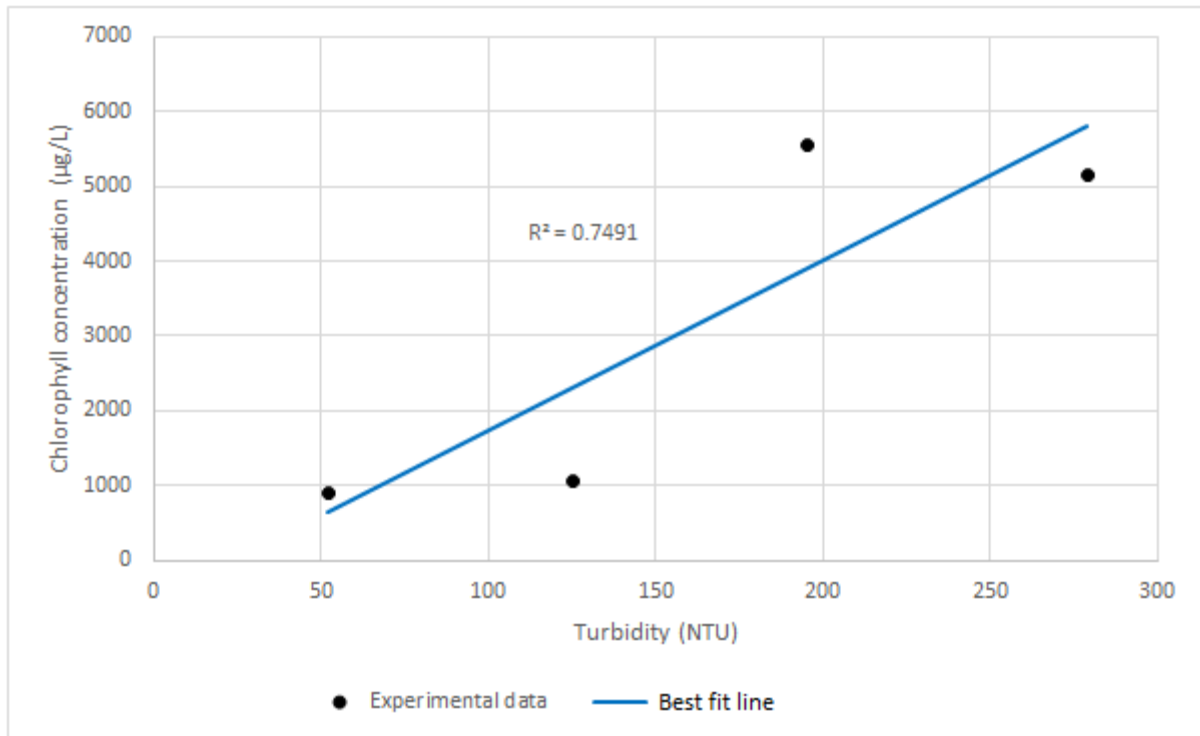


Figure 41. Correlation between turbidity and chlorophyll a concentration.

As shown in figure 41, the curve is not perfectly suited to the experimental values as R^2 is 0.75. However, from a statistical point of view there is a dependency between turbidity and chlorophyll concentration, therefore, the maximum concentration values obtained in the non-linear regression analysis can be expressed in terms of chlorophyll concentration, i.e., $\mu\text{g/L}$.

Experiment 2

In order to obtain a large volume of culture, flask 3 was chosen to further develop of more algae (under same conditions), because under this CO_2 percentage (15%), algae best adapted to the medium and had a high chlorophyll and biomass concentration. It is important to highlight that fuel-burning electric powers plants, emit only between 3 and 15% CO_2 , which means that 100% of the emissions from such a source would be taken advantage of by algae growth, with the subsequent benefit of energy conversion. This would result in a decrease in the concentrations of CO_2 in the atmosphere, which means a significant reduction of global warming.

Table 9 shows the exhaust gases composition by volume (%v/v) from different fuel-burning electric powers plants; from this table it can be seen that CO_2 emissions ranges from 3% (gas fired) to 15% (coal firing).

Table 9. Exhaust gases composition by volume (%v/v). SOURCE: (The k2p blog, 2013) www.ktwop.com

	Air (wet)	Coal firing	Bio-mass combustion	petrol fired IC engine	diesel fired IC engine	Gas fired GT combined cycle	Human breath
Nitrogen N_2 (mw 28)	77.3	69 to 73	c.66	72	66	74 to 78	77 to 78
Oxygen O_2 (mw 32)	20.7	5 to 6	c. 8	0	10	13 to 14	15
Carbon Dioxide CO_2 (mw 44)	0.039	11 to 15	c. 10	14	12	3 to 5	4
Water vapour H_2O (mw 18)	1.0	10 to 12	c. 15	13	11	to 6	2 to 3
Argon Ar (mw 40)	0.93	1	1		1	1	1
Carbon monoxide CO (mw 28)	0	0	0	1	0	0	0

Experiment 3

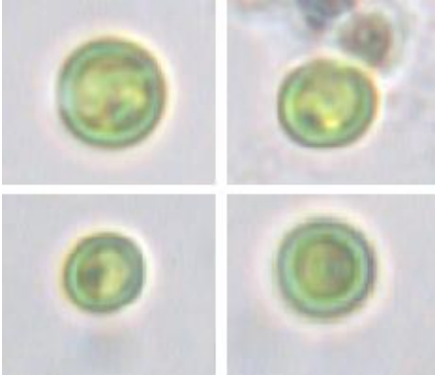
The cell wall of *Chlorella Vulgaris* microalgae, is considered one of the strongest, since it is able to coexist in places with high concentrations of pesticides, toxins and heavy metals in addition to resist fermentation processes.

For energy production through algae biomass digestion, one of the most feasible process is anaerobic digestion, as this produces biogas from wet stream and requires less energy than thermochemical processes. In addition to this, the biogas produced contains between 55 and 75% methane, which can be burned to produce heat and/or electricity. However, to carry out this process, it is necessary an effective pretreatment to break the algae cell walls so the biomass is made available during digestion. The premise of such treatment is to supply energy to an algal culture to rupture (lyse) the cells.

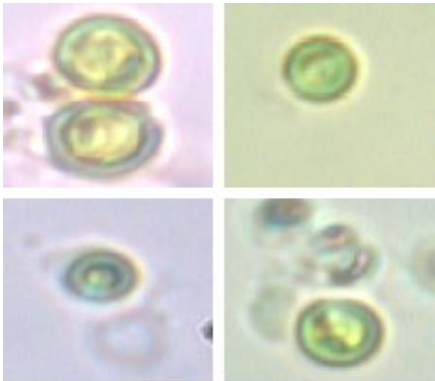
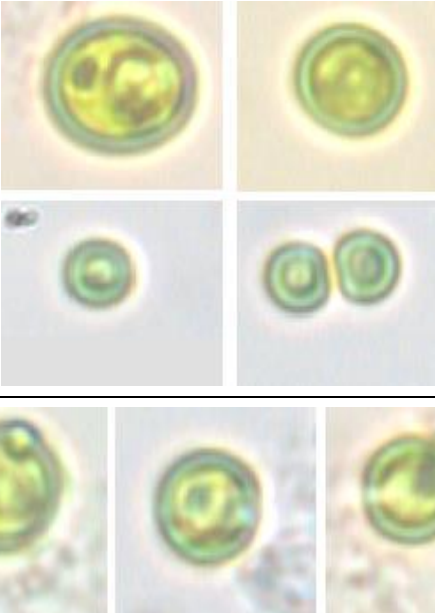
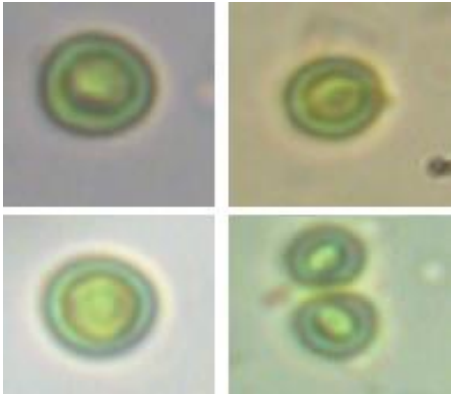
a. Electroporation experiment using constant voltage

A constant voltage of 30, 47.5 and 65V, was applied to the algae sample during different detention times; the following results were obtained:

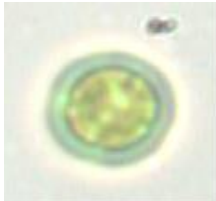
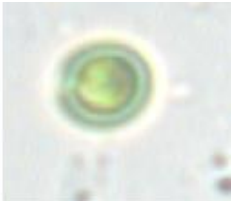
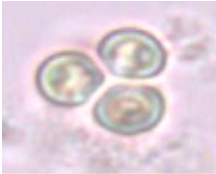
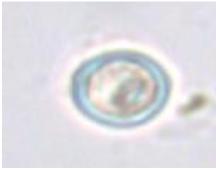
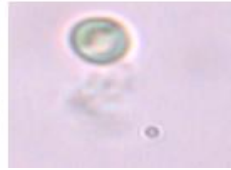
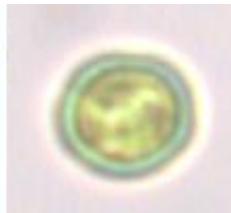
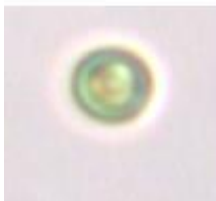
Table 10. Constant voltage mode results.

Constant voltage mode				
Voltage (Volts)	Time	Current (Amp)	Conductivity ($\mu\text{S}/\text{cm}$)	Cell wall
30	1 min	1.5	1557	

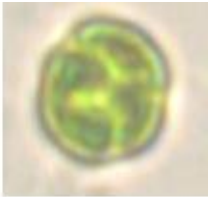
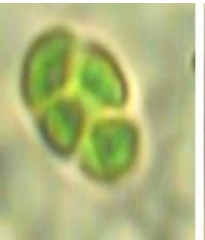
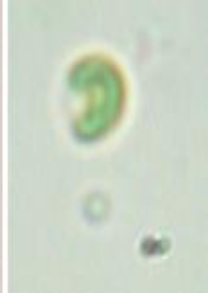
(Table 10 continued)

Voltage (Volts)	Time	Current (Amp)	Conductivity ($\mu\text{S}/\text{cm}$)	Cell wall
30	2 min	1.5	1559	
30	5 min	1.7	1559	
47.5	1 min	3	1564	

(Table 10 continued)

Voltage (Volts)	Time	Current (Amp)	Conductivity ($\mu\text{S}/\text{cm}$)	Cell wall	
47.5	3 min	3.3	1564		
47.5	5 min	3.6	1554		
					
65	30 secs	3.9	1557		
					

(Table 10 continued)

Voltage (Volts)	Time	Current (Amp)	Conductivity ($\mu\text{S}/\text{cm}$)	Cell wall		
65	1 min	3.9	1562			
65	2 min	5	1560			
65	3 min	5.1	1560			
65	4 min	7.6	1560			
65	5 min	8.9	1560			

From Table 10, it can be seen that for 30 volts and a short detention time, of 1 to 2 minutes, the cell wall remained intact, however, when the detention time increased to try to achieve a rupture, there was a small break only in some cell's membranes.

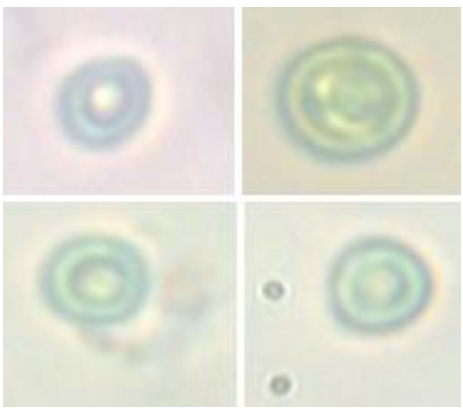
The same applies when the voltage increased to 47.5 volts, when detention time reached 3 minutes, a small opening in the cell wall was observed, however, for 5 minutes, most of the cells remained intact, except a few, where the wall was completely broken.

When a voltage of 65 volts was applied to the sample, it was observed that the wall remained intact for the first 30 seconds, however, for a detention time of 1 minute, a complete break was observed, which increased with detention time. After 5 minutes, a complete destruction of the cell wall in conjunction with the spread of protoplasm was observed.

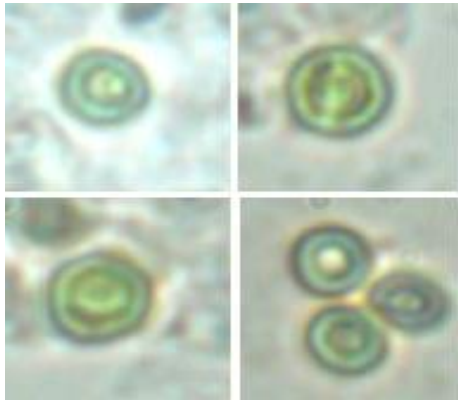
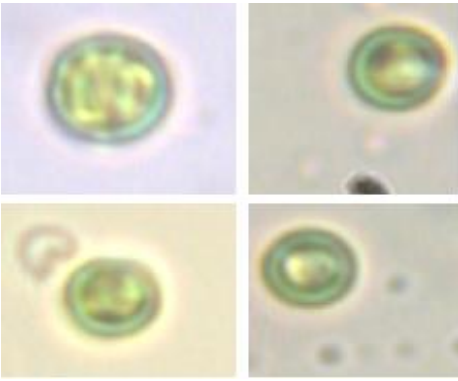
b. Electroporation using constant current

A constant current of 5.4 and 10.8 Amp, was applied to the algae sample during different detention times; the following results were obtained:

Table 11. Constant current mode results.

Constant current mode					
Current (Amp)	Time	Voltage (Volts)	Initial Conductivity ($\mu\text{S}/\text{cm}$)	Final Conductivity ($\mu\text{S}/\text{cm}$)	Cell wall
10.8	1 min	38.7	1572	5660	

(Table 11 continued)

Current (Amp)	Time	Voltage (Volts)	Initial Conductivity ($\mu\text{S}/\text{cm}$)	Final Conductivity ($\mu\text{S}/\text{cm}$)	Cell wall
10.8	2 min	36.4	1582	5300	
10.8	4 min	32	1580	5230	
5.4	1 min	29.1	1580	5730	

As shown in Table 11, for a current of 5.4 and 10.8 amperes, and short detention time of around 2 minutes, the cell wall suffered no break. However, when the detention time increased to 4 minutes, it was observed that a few cells, suffered a small break.

- Temperature test

In table 12, an increment in the temperature of more than double was observed when constant current was used; also, under this mode, for any detention time, gases and water vapor escaped from the reactor (Figure 42), and the cell wall breaking only worked for a few cells using the highest current and detention time. Therefore, the constant current was not considered an effective treatment for breaking the cell wall of algae.

Table 12. Temperature results.

Time	Voltage (Volts)	Current (Amp)	Initial temperature (°C)	Final temperature (°C)	Initial Conductivity (µS/cm)	Final Conductivity (µS/cm)
1 min	65	3.9	18.9	23	1633	1886
5 min	65	8.9	18.9	27	1800	1671
1 min	38.7	10.8	19.5	54	1553-5180	5000
4 min	32	10.8	19.5	56.2	1553-5180	4984

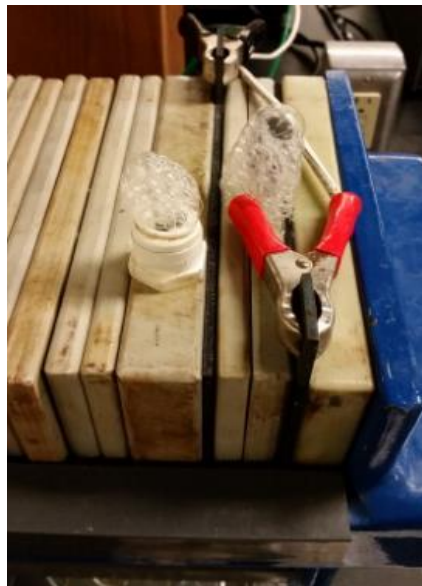


Figure 42. Gases and water vapor.

The most feasible and economic treatment is the one that meets the objective of breaking the cell wall permanently of all the algae present in the sample, with less energy used and the shortest detention time, therefore, as shown in table 10, the best arrangement was to use a constant voltage of 65 volts with a current of 3.9 amps for a period of 1 minute.

It is important to highlight, that cell wall break was due solely to electricity (using titanium electrodes coated with iridium oxide). No chlorine generation was possible because the growth medium did not have any chlorides.

Chapter V

Conclusions and Recommendations

Conclusions

As part of research looking into using algae as source of biomass for energy production, the growth of microalgae *Chlorella vulgaris* was studied in this research. This was done by using a shaking water bath for 10 weeks to grow the algae under different CO₂ percentages. A batch reactor (with titanium electrodes) connected to a direct current (DC) power supply was used for the subsequent electroporation of their cell wall. Temperature, conductivity, pH, turbidity and alkalinity were measured during all phases of experiment.

CO₂ concentration is one of the fundamental factors affecting algae growth. Therefore, as shown in Figures 29 to 40, for 0% CO₂ no growth was observed, for 5 and 10%, growth rate was high with a very low maximum concentration; for 15% CO₂, growth was slow but had a high chlorophyll and population concentration, and for 20%, growth was progressive but took longer.

Therefore, the maximum CO₂ concentration that can be added to a suspension of *Chlorella vulgaris* within the emission range from thermoelectric plants, was 20%. However, the optimal dose for highest algae and chlorophyll concentration was 15% CO₂, under a pH of 6.64 and a final alkalinity of 617.5 mg/L as CaCO₃.

In order for algae to be suitable for use as biomass for energy, pretreatment to break its cell wall is necessary; for that reason, an electrochemical batch reactor equipped with titanium electrodes and current supplied by a DC regulated power supply was used, which has a high efficiency under the study conditions.

After analyzing the data obtained in tables 10 and 11, the following parameters demonstrated to have a relationship with the reactor efficiency:

- Detention time of 1 ± 0.5 minutes.
- Minimum voltage of $65 \frac{\text{Volts}}{285 \text{ ml}}$
- Minimum current of $3.9 \frac{\text{Amps}}{285 \text{ ml}}$

The combination of the three recommended parameters yielded visible and permanent cell wall break. The energy input is very small and has the capability to become self-sustained if renewables energies are implemented.

The electrochemical batch reactor caused a significant increase in temperature when constant current was applied, as opposed to slight temperature increase with constant voltage. Table 12 and Figure 42 show an increase of more than double and the production of large amounts of gases and water vapor, respectively.

Algal breakage under constant voltage was due to electrocution only, because the growth medium lacked chlorides, so chlorine generation was not possible.

Recommendations

- Based on the results of this research, it is recommended to not interconnect the bottles to each other to prevent evaporation of the sample, since not only the air is being transmitted between them, but also CO_2 .
- For better results, it is recommended to previously mix the CO_2 with the air, and inject the mixture of both, to each sample.

- In order to obtain a more precise estimate of algae concentration without sample wasting, it is recommended to measure its absorbance. Due to the presence of photosynthetic pigments, it is important to conduct the measurement outside of the range of wavelengths where these pigments absorb, that is, at 550 nm (Becker, 1994).
- When evaporation in the culture is present, the amount spent should be replaced with water and not with medium, as the chemical components thereof greatly increase the alkalinity.
- For a further analysis of energy production through algae biomass treatment using anaerobic digestion, it is necessary to use a continuous flow reactor; for this, the cultivation of a large volume of algae for obtaining a minimum flow rate of 17.1 L/h or $4.75 \times 10^{-6} \text{ m}^3/\text{s}$ within the reactor, is recommended.
- Measure dissolved solids to determine what causes the increase and decrease in conductivity when applying constant voltage.
- Establish a correlation between chlorophyll concentration and turbidity, and another correlation between absorbance and chlorophyll concentration, to determine which of the two parameters is more representative in the estimation of chlorophyll concentration and therefore in algae growth.

Chapter VI

References

- Al-Qasbi, M. T. (2012). A Review of Effect of Light on Microalgae Growth. *Proceedings of the World Congress on Engineering*, Volume I.
- Arredondo, B. V.-D. (1991). Aplicaciones biotecnologicas en el cultivo de microalgas. *Ciencia y Desarrollo*, 17, 99 - 111.
- Becker, E. W. (1994). *Microalgae: Biotechnology and Microbiology*. Cambridge, U.K.: Cambridge University Press.
- Bilanovic, D. A. (2009). Freshwater and marine microalgae sequestering CO₂ at different C and N concentrations-Response surface methodology analysis. *Energy Conversion and Management*, 50, 262 - 267.
- Biofuels, C. o. (2012). *Sustainable Development of Algal Biofuels in the United States*. Washington, D.C.: The National Academies Press.
- Bittencourt, E. (2009). *Respirometric balance and analysis of four microalgae: Dunaliella tertiolecta, Chlorella vulgaris, Spirulina platensis and Botryococcus braunii*.
- Borowitzka, M. (1999). Commercial production of microalgae: ponds, tanks, tubes and fermenters. *Journal of Biotechnology*, 70, 313 - 321.
- Brendan, M. O. (2010). Biofuels from microalgae - A review og tchnologies for production, processing, and extraction of biofuels and co-products. *Renewable and Sustainable Energy Reviews*, 14, 557 - 577.
- CEES, C. f. (n.d.). Retrieved from What causes algal blooms?: <http://www.cees.iupui.edu/research/algal-toxicology/bloomfactors>
- Cheirsilp, B. T. (2012). Enhanced growth and lipid production of microalgae under mixotrophic culture condition: Effect of light intensity, glucose concentration and fed-batch cultivation. *Bioresource Technology*.
- Chinnasamy, S. R. (2009). Biomass production potential of a wastewater Alga Chlorella vulgaris ARC 1 under elevated levels of CO₂ and temperature. *International Journal of Molecular Sciences*, 10, 518 - 532.
- Chisti, Y. (2007). Biodiesel from Microalgae. *Biotechnology Advances*, 25, 294 - 306.
- Chisti, Y. (2008). Biodiesel from microalgae beats bioethanol. *Trends Biotechnology*, 26: 126 - 131.
- Dalrymple, O. H. (2013). Wastewater use in algae production for generation of renewable resources: a review and preliminary results . *Aquatic Biosystems*, 9: 2.
- De Grau, L. (2015). *Electrochemical Disinfection of Municipal Wastewater*. New Orleans: University of New Orleans.
- EIA. (2016). *Energy-related CO₂ emissions*. U.S. Energy Information Administration.
- FAO. (2009). *Algae-based biofuels: A review of Chanllenges and Opportunities for Developing Countries*. Roma.
- Flinn Scientific, I. (2012). *Culturing Algae, Live Material Care Guide*. Batavia, IL: Flinn Scientific Inc.

- Fulke, A. C. (2013). Potential of wastewater grown algae for biodiesel production and CO₂ sequestration. *African Journal of Biotechnology*, 12, 2939 - 2948.
- Fulke, A. M. (2010). Bio-mitigation of CO₂, calcite formation and simultaneous biodiesel precursors production using *Chlorella* sp. *Bioresource Technology*, 101, 8473 - 8476.
- Garcia, M. J. (2010). *Captura de CO₂ mediante algas unicelulares*. Madrid: Universidad Politecnica de Madrid.
- Garibay, A. V. (2009). Biodiesel a Partir de Microalgas. *BioTecnologia*, Vol. 13, No 3. pp. 51 - 55.
- Gilles, S. L. (2008). Mutualism between euryhaline tilapia *Sarotherodon melanotheron* heudelotii and *Chlorella* sp.- Implications for nano-algal production in warmwater phytoplankton-based recirculating systems. *Aquacultural Engineering*, 39(2-3), 113 - 121.
- Golueke, C. O. (1956). Anaerobic Disgestion of Algae. *Applied Microbiology*, 47 - 55.
- Hamilton, W. S. (1967). Effective of high electric fields on microorganisms: II. Mechanisms and action of the lethal effect. *Biochimica et Biophysica, Acta* 148, 789 - 800.
- Henry, H. H. (1999). *Ingenieria Ambiental*. Mexico: Pearson Educacion.
- Heredia, T. W. (2011). Mixotrophic cultivation of *Chlorella vulgaris* and its potential application for the oil accumulation from non-sugar materials. *Biomass Bioenergy*, 35, 2245 - 2253.
- Hernandez, A. e. (2009). Biodiesel a Partir de Microalgas. *Biotechnologia y Bioingenieria*, 13, 38 - 61.
- Hoffman, J. (1998). Wastewater treatment with suspended and nonsuspended algae. *Journal of Phycology*, 34, 757 - 763.
- Kanduser, M. M. (2009, February). *Electroporation in Biological Cell and Tissue: An Overview*. University of Ljubljana. Retrieved from <http://lbk.fe.uni-lj.si/pdfs/eefp2008.pdf>
- Karcher, K. (2010). *Optimization of environmental conditions to maximize carbon dioxide sequestration through algal growth*. Ohio: Department of Air Force, Air University, Air Force Institute of Technology.
- Kentucky Water Watch. (n.d.). Retrieved from Total Suspended Solids and Water Quality. In River Assessment Monitoring Project: <http://ky.gov/nrepc/water/ramp/rmtss.htm>
- Khoeyi, Z. S. (2011). Effect of light intensity and photoperiod on biomass and fatty acid composition of the microalgae. *Springer science+ Business Media*.
- Kin, S. (2010, November 23). *Biofuels Project 2010*. Retrieved from <http://biofuels2010.blogspot.com/2010/11/manufacturing-processes-of-algae.html>
- Kinosita, K. T. (1979). Voltage induced conductance in human erythrocyte membranes. *Biochimica et Biophysica, Acta* 554, 479 - 497.
- Kitaya, Y. A. (2005). Effects of temperature CO₂/O₂ concentrations and light intensity on cellular multiplication of microalgae, *Euglena gracilis*. *Advances in Space Research*, Volume 35, Issue 9, Pages 1584 - 1588.
- Koning, R. (1994). *Plant physiology information website*. Retrieved from http://plantphys.info/plant_physiology/calvincycle.shtml
- Lebovka, N. B. (2002). Estimation of characteristics damage time of food materials in pulse-electric fields. *Journal of Food Engineering*, 54, 337 - 346.
- Lee, A. L. (2009). Microbial flocculation, a potentially low-cost harvesting technique for marine microalgae for the production of biodiesel. *Journal of Application of Phycology*, 21: 559 - 567.

- Lee, R. D. (2003). Electrical injury: mechanisms, manifestations and therapy. *IEEE Transactions on Dielectrics and Electrical Insulation*, 10, 810 - 819.
- Liu, J. S. (2014). *Recent Advantages in Microalgal Biotechnology*. Foster City: OMICS Group eBooks.
- Madrid, A. (2009). Energías Renovables: Fundamentos, tecnologías y aplicaciones. *Mundi-Prensa*, 379.
- Malgas. (2013). *Aplicaciones de las microalgas: estado de técnica*. Asturias: AST Ingeniería S.L.
- Mara, D. P. (1998). *Design Manual for Waste Stabilization Ponds in Mediterranean Countries*. Leeds, England: Lagoon Technology International.
- Neumann, E. S. (1989). *Electroporation and electrofusion in cell biology*. New York: Plenum Press.
- Norihiro, S. M. (2003). Glycerolipids synthesis in *Chlorella kessleri* 11 h II. Effect of the CO₂ concentration during growth. *BBA Molecular and Cell Biology of Lipids*, 1633(1), 35 - 42.
- OpenStax. (2013). *Concepts of Biology*. OpenStax, OpenStax Concepts of Biology.
- Oswald, W. G. (1957). *Photosynthesis in sewage treatment*. American Society of Civil Engineers.
- Oswald, W. J. (1990). Advanced integrated wastewater pond systems. *Proceedings of the ASCE convention: Supplying water and saving the environment for six billion people.*, (pp. 73 - 80). San Francisco, CA.
- Perlman, H. (2014, March). Retrieved from The USGS Water Science School: <http://water.usgs.gov/edu/turbidity.html>
- Ramanan, R. K. (2010). Enhanced algal CO₂ sequestration through calcite deposition by *Chlorella* sp. and *Spirulina platensis* in a mini-raceway pond. *Bioresource and Technology*, 101(8), 2616 - 2622.
- Richmond, A. (1986). Microalgal culture. *CRC, Critical Reviews in Biotechnology*, 369 - 438.
- Richmond, A. (2004). *Handbook of microalgal culture: Biotechnology and applied phycology*. UK: Ed. Blackwell Science LTD.
- Rincon, G. L. (2013). Kinetics of Electrocoagulation of Hexane Extractable Materials. *Journal of Ship Production and Design*, 57 - 65.
- Rochet, M. L. (1986). Quality. *Journal of Experimental Marine Biology and Ecology*, Volume 101, Issue 3, 4, Pages 211- 226.
- Rodolfi, L. Z. (2009). Microalgae for Oil: Strain Selection, Induction of Lipid Synthesis and Outdoor Mass Cultivation in a Low-Cost Photobioreactor. *Biotechnology and Bioengineering*, 102: 100 - 112.
- Rodriguez, D. D. (2009, Abril 14). *Biotechnología de la producción de algas*. Retrieved from <http://biotecprodalgas.blogspot.com/>
- Rols, M. (2006). Electroporation, a physical method for the delivery of therapeutic molecules into cells. *Biochimica et Biophysica Acta* 1758, 423 - 428.
- Safi, C. B. (2014). Morphology, composition, production, processing and applications of *Chlorella vulgaris*: A review. *Renewable and Sustainable Energy Reviews*, 35: 265 - 278.
- Santra, T. W. (2013). *Electroporation Based Drug Delivery and Its Applications, Advances in Micro/Nano Electromechanical Systems and Fabrication Technologies*. InTech.
- Schenk, P. T.-H. (2008). Second generation biofuels: high-efficiency microalgae for biodiesel production. *Bioenergy Resource*, 1: 20 - 43.

- Singh, S. (2014). Effect of CO₂ concentration on algal growth: A review. *Renewable and Sustainable Energy Reviews*, 174.
- Stenger, D. H. (1986). Kinetics of ultrastructural changes during electrically-induced fusion of human erythrocytes. *The Journal of Membrane Biology*, 93, 43 - 53.
- Stepan, D. S. (2002). *Carbon dioxide sequestering using microalgae system*. Pittsburgh, PA: US Department of Energy.
- Stephens, E. R. (2010). Future prospects of microalgal biofuel production systems. *Trends in plant science*, 15, 554 - 564.
- Teissie, J. E. (2002). Recent biotechnological developments of electropulsation: A prospective review. *Bioelectrochemistry*, 5, 107 - 112.
- Testo. (2004). *Flue Gas Analysis in Industry*. Germany: Testo.
- The k2p blog. (2013, April 13). Retrieved from <https://ktwop.com/tag/flue-gas-composition/>
- Ugwu, C. A. (2007). Photobioreactor for mass cultivation of algae. *Bioresource Technology*, 99, pp. 4021 - 4028.
- Ugwu, C. A. (2008). Photobioreactors for mass cultivation of algae. *Bioresource Technology*, 99, 4021- 4028.
- Van Den Hende, S. C. (2014). Treatment of industrial wastewaters by microalgal bacterial flocs in sequencing batch reactors. *Bioresource Technology*, 245 - 254.
- Viswanathan, T. S. (2011). Drying characteristics of a microalgae consortium developed for biofuels production. *Transactions of the ASABE*, 54(6): 2245 - 2252.
- Wang, B. L. (2008). CO₂ bio-mitigation using microalgae. *Application Microbiology Biotechnology*, 79, 707 - 718.
- Ward, A. L. (2014). Anaerobic digestion of algae biomass: A review. *Algal Research*, 204 - 214.
- Weaver, J. C. (1996). Theory of electroporation. *Bioelectrochemistry and Bioenergetics*, 41, 135 - 160.
- Wegmann K, M. H. (1971). Synchronization of *Dunaliella salina* cultures. *Archives of Microbiology*, 78: 360-367.
- Wijffels, R. (2010, 08 04). *Presentation Microalgae for production of energy*. Retrieved from http://www.worldbiofuelsmarkets.com/downloads/presentations/Algae_15th/rene_wi
- Wood, A. M. (2005). *Measuring growth rates in microalgal cultures*. Burlington, MA: Elsevier Academic Press: Ed. R. A. Andersen.
- Zevenhoven, R. K. (2002). *Control of pollutants in flue gases and fuel gases*. Espoo/Turku, Finland: Helsinki University of Technology.
- Zhang, Q. B.-C. (1995). Engineering aspects of pulsed electric field pasteurization. *Journal of Food Engineering*, 25, 261 - 281.
- Zimmermann, U. (1982). Electric field-mediated fusion and related electrical phenomena. *Biochimica et Biophysica Acta* 696, 227 - 277.

Chapter VII

Appendix

Appendix A: Detailed explanation of laboratory methods.

a. Medium preparation for algae growth

Laboratory equipment:

- OHAUS Precision Standard Balance
- Fisher Scientific Thermo® Stirrer Model 120S magnetic stirrer
- Magnetic stir bar
- Graduated cylinder
- Aluminum petri dish
- 1 L Beaker

Reagents:

- Flinn Scientific Inc., Bristol's algae media concentrate 100 X
- EM Calcium carbonate GR 500 g
- EMD® Sodium bicarbonate GR ACS 500 g
- Unfertilized soil
- Deionized water

Procedure:

10 ml of Bristol's medium (Figure 43) were added to the beaker, then was filled with deionized water until 1-L mark and added 2 pinches of soil. Then, 20 mg of Calcium Carbonate

and 250 mg of Sodium Bicarbonate were measured in the precision balance and added to the mix.



Figure 43. Bristol's Algae Media.

The stir bar was added to the beaker, and placed on top on a magnetic stirrer, mixed until homogenous mix was achieved (Figure 44).



Figure 44. Well-mixed medium.

b. pH and Conductivity

Laboratory equipment:

- Thermo Scientific Orion 5 Star™ Plus Meter
- Thermo Orion pH meter model 410
- Fisher Scientific Thermo® Stirrer Model 120S magnetic stirrer
- Magnetic stir bar
- Different capacity beakers

Reagents:

- Acros, Buffer solution – pH 4.0 color coded red
- Acros, Buffer solution – pH 7.0 color coded yellow
- Acros, Buffer solution – pH 10.0 color coded blue
- YSI 3163 Conductivity Calibrator
- YSI 3161 Conductivity Calibrator
- Deionized water

Procedure:

pH

For pH measurements two different pH meters were used. The first step was calibrating each pH meter. For pH calibration of Orion Star™, the arrow icon must be pointed to pH in the screen. Then, the “Calibrate” button was pressed. The electrode must be rinsed with deionized water, dried with a tissue, and then placed in a 4.0 buffer solution.

A few time had to be allowed so the AR icon in the display became stable. If the pH reading was out of range, the correct number was entered manually. After this, the “calibrate” button was pressed again to continue with the following calibration point. The electrode was removed from the 4.0 buffer solution, rinsed with deionized water, dried with a tissue and placed in a 7.0 buffer solution. The procedure is the same for the remaining buffer solution.



Figure 45. Buffer solutions for pH meter.

In order to take actual measurements in the Orion Star™ Plus Meter (Figure 46), the electrode was rinsed with deionized water, dried with a tissue, and placed into the sample. To make a reading, it is necessary to press “Line Select” until the arrow icon points to the pH icon, and then press “Measure Save/Print”.



Figure 46. Orion Star™ Plus Meter.

A beaker containing a magnetic stirrer and the sample to be analyzed was placed on a magnetic plate, so the solution was well mixed and the pH reading was accurate.

For pH calibration of Thermo Orion, the electrode was connected to the meter, rinsed and placed in the buffer. The “mode” button was pressed until “CALIBRATE” was displayed. The last buffer sequence used was displayed, then the “yes” button was pressed to use that sequence (the “no” button can be pressed to scroll through choices).

Buffer indicator along bottom of the display indicated the buffer chosen. P1 was displayed in lower display field and buffer reading was displayed in the main field. When “READY” was displayed, indicating electrode stability, the “no” button was pressed to change each digit until the correct pH value was displayed then “yes” was pressed to accept.

The temperature corrected value for that buffer was automatically entered into the memory of the meter. P2 was displayed in the lower display field indicating the meter was ready for the second buffer. The buffer indicator along the bottom of the display indicated the second buffer of the calibration sequence selected.

The previous steps were repeated for each buffer. After the buffer value for the last buffer was entered, “measure” button was pressed. The electrode slope was displayed. “SLP” appeared in the lower field while the actual electrode slope, in percent, appeared in the main field. “yes” button was pressed; the meter was automatically advance to the measure mode. “MEASURE” was displayed above the main field.

In order to take actual measurements in the Thermo Orion pH meter (Figure 47), the electrode was rinsed and placed into sample and the pH was recorded directly from the main meter display when “READY” was displayed. A beaker containing a magnetic stirrer and the sample to be analyzed was placed on a magnetic plate, so the solution was well mixed and the pH reading was accurate.



Figure 47. Thermo Orion pH meter.

Conductivity

For calibration of the conductivity meter, the arrow icon must be pointed to the conductivity icon, and then press “Calibrate” to start calibration. The conductivity probe was rinsed with deionized water, dried with a tissue, and placed in the conductivity calibrator solution 1000 $\mu\text{S}/\text{cm}$. Several minutes had to be allowed so the AR icon in the display became stable. Afterward, the “calibrate” button was pressed to continue with the following calibration point. The conductivity probe was removed from this solution, rinsed, dried and placed in the conductivity calibrator solution 10,000 $\mu\text{S}/\text{cm}$.



Figure 48. Conductivity calibration standards.

For actual conductivity measures, the conductivity probe was rinsed with deionized water, dried with a tissue, and placed into the sample (Figure 49). The “Line Select” button in the Orion Star™ Plus Meter was pressed until the arrow icon points to the conductivity icon, and then the icon “Measure Save/Print” was pressed to make a reading. A beaker containing a magnetic stirrer and the sample to be analyzed was placed on a magnetic plate, so the solution was well mixed and the pH reading was accurate.

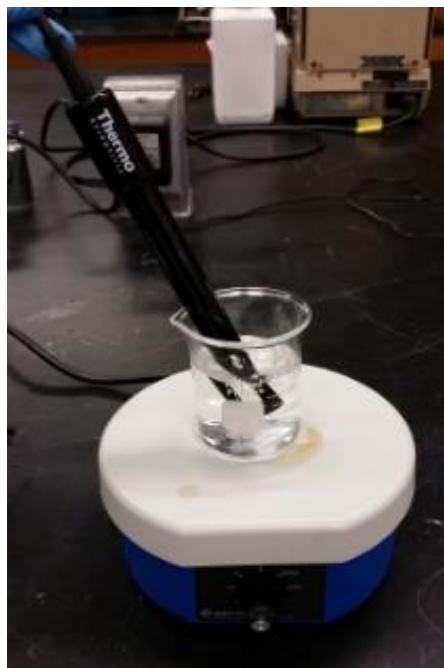


Figure 49. Conductivity probe.

c. Alkalinity

Laboratory Equipment:

- Thermo Orion pH meter model 410
- Fisher Scientific Thermo® Stirrer Model 120S magnetic stirrer
- Magnetic stir bar
- 50 ml Burette

- 100 ml beaker
- Burette holder
- Graduated cylinder

Reagents:

- HACH, Cat. 20353, Sulfuric Acid Standard Solution 0.020N, 1000 ml
- HACH Permachem Reagents, Cat. 94399 Pk/100, Bromcresol Green-Methyl Red Indicator Powder.
- Deionized water

Procedure:

The pH meter was calibrated, after that, 40 ml of each sample was poured into the beaker with a stir bar inside, and then placed on top of the magnetic plate to mix the solution at a speed of 370 rpm (constant).

Afterwards, 50 ml of sulfuric acid solution was poured into the burette and placed in the burette holder above of the magnetic plate with the sample solution. Later the pH meter was placed inside the solution to measure at all times. Before starting the titration, 1 bag of Bromcresol Green-Methyl Red indicator was added to the solution.

Then, the titration was started by adding 1 ml (around 3-4 drops) of titrant (H_2SO_4) to the sample (40 ml) until reached the color of the indicator (pink) at established pH (around 4.5). Volume of acid added and pH of sample was recorded at all times.



Figure 50. Alkalinity indicator end point (Pink).

The following equation was utilized to calculate the test results:

$$\text{Alk} \left(\frac{\text{mg}}{\text{L}} \text{ as CaCO}_3 \right) = \frac{V * N}{\text{Sample volume}} * 50000 \frac{\text{mg CaCO}_3}{\text{eq}} \quad (17)$$

Where:

V = Volume of titrant spent, ml

N = Normality of titrant, N

d. Calcium

Laboratory Equipment:

- Thermo Orion pH meter model 410
- Fisher Scientific Thermo® Stirrer Model 120S magnetic stirrer
- Magnetic stir bar

- 50 ml Burette
- 100 ml beaker
- Burette holder
- Graduated cylinder

Reagents:

- HACH, Cat. 205-53, TitraVer (EDTA) Standard Solution 0.010 M (0.020 N)
- HACH, Cat 282-32H, Potassium Hydroxide Solution 8 N
- HACH Permachem Reagents, Cat. 85299 Pk/100, CalVer 2 Calcium Indicator Powder
- Deionized water

Procedure:

The pH meter was calibrated, after that, 50 ml of each sample was poured into the beaker with a stir bar inside, and then placed on top of the magnetic plate to mix the solution at a speed of 370 rpm (constant).

Afterwards, 50 ml of EDTA standard solution was poured into the burette and placed in the burette holder above of the magnetic plate with the sample solution. Later the pH meter was placed inside the solution to measure at all times. Before start the titration, the pH was first adjusted to 10 using 1 ml of KOH and then 1 bag of CalVer 2 indicator was added to the solution.

Then, the titration was started by adding 1 ml (around 3-4 drops) of titrant (EDTA) to the sample until reached the color of the indicator (pure blue). Volume spent and pH of sample was recorded.

The method used to calculate the calcium of the samples was HACH 8222, which states that calcium is calculated by multiplying the amount of titrant spent by 20, when the sample volume is 50 ml and the normality of the titrant is 0.02 N.

The calculation is based on an equation written as if all the hardness were due to calcium carbonate. The reaction is 1 mol to 1 mol.

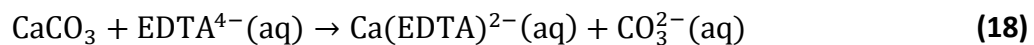


Figure 51. Calcium indicator end point (Blue).

e. Turbidity

Laboratory Equipment:

- HF Scientific Micro 100 Turbidimeter
- Cuvettes
- Beaker

Reagents:

- Calibration set for Micro 100 Turbidimeter: 1000, 10 and 0.02 NTU calibration standard.

Procedure:

The first step was calibrating the turbidimeter (Figure 52), for that, the “CAL” button was pressed; then the 1000 NTU standard was placed into the turbidimeter and finally the “Enter” button (arrow pointing to the left) was pressed. The same procedure was repeated using the 10 and 0.02 NTU calibration standard solutions (Figure 53).



Figure 52. Turbidimeter.



Figure 53. Turbidimeter calibration set.

Once the last standard solution was taken from the turbidimeter, the calibration was done. Each sample was poured into a beaker and then poured into a clean cuvette three times to rinse it. After this, the cuvette was filled with the sample, covered with a cap and dried, then was placed in the optical well and indexed to the lowest reading.

To ensure that the reading was correct, the sample was slowly rotated until complete one revolution (360°).

Same procedure was done for all samples.

f. Chlorophyll A

Laboratory Equipment:

- Eppendorf Centrifuge 5810 R
- DR 5000™ UV-Vis HACH Spectrophotometer
- Fisher Scientific Thermo® Stirrer Model 120S magnetic stirrer
- Filtration Apparatus
- 10 mm HACH Quartz Cells
- Glass Fiber Filters
- Conical Centrifuge Tubes
- Magnetic stir bar
- Pipettes
- Aluminum Foil
- Fridge

Reagents:

- Fisher Chemical Acetone Certified ACS (99.7%)
- Deionized water

Procedure:

For the Wegmann-Metzner method of chlorophyll determination, a 90% acetone solution was needed, therefore, the first step was made 50 ml of 90% acetone using 4.9 ml of deionized water and 45.1 ml of 99.7% acetone.

Afterward, the filtering apparatus was assembled, the vacuum was turned on, the filter (wrinkle side up) was placed on top of the apparatus and the last part of the filtering was assembled (Figure 54).



Figure 54. Filtering Apparatus completely assembled.

The samples were well mixed using a magnetic stir plate, and then using a pipette, 5 ml were taken from each sample and filtered (separately). Each filter was placed into a 15 ml conical centrifuge tube containing 5 ml of 90% acetone (Figure 55). Tubes were covered with aluminum foil and kept in the fridge at 4 °C for 24 hours.

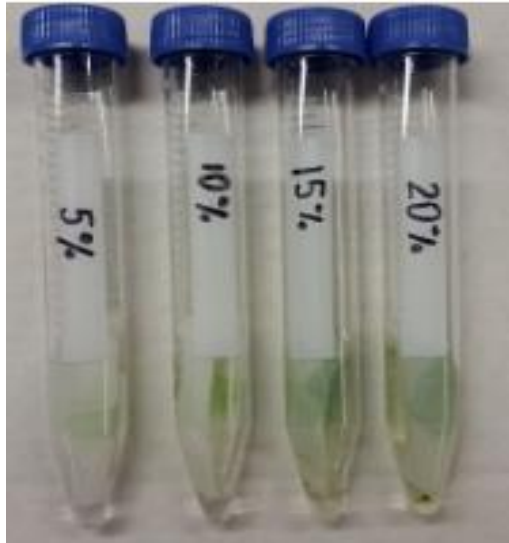


Figure 55. Tubes with filter and acetone.

The next day, samples were shaken and centrifuged at 3500 rpm for 5 minutes (Figure 56), and the extracts were read in the spectrophotometer at 750, 663 and 644 nm.



Figure 56. Samples inside the centrifuge.

For the Chlorophyll calculations, the absorbance lectures had to be corrected for turbidity using the following formulas:

$$E_{663} = E_{663} - E_{750} \quad (19)$$

$$E_{644} = E_{644} - E_{750} \quad (20)$$

Where E_{663} , E_{644} and E_{750} are the absorbance at 663, 644 and 750 nm respectively.

To calculate the relative concentration of chlorophyll a, the following equation was used:

$$C_{\text{Chloro a}} = 10.3 * E_{663} - 0.981 * E_{644} \quad (21)$$

Finally, to calculate the pigment concentration per volume of culture in $\mu\text{g/L}$ or mg/m^3 , the following equation was used:

$$\text{Chlorophyll a } \left(\frac{\mu\text{g}}{\text{L}} \right) = \frac{C_{\text{Chloro a}} * v}{V * z} \quad (22)$$

Where:

v = Volume of extract, ml

V = Volume of culture, L

z = Light path length, cm

g. Cell wall break

Laboratory Equipment:

- Ecolotron reactor
- BK Precision High Current DC Regulated Power Supply, Model 1791
- ENERPAC P39 Hydraulic Jack

- OMANO OMFL400 Fluorescence Compound Microscope
- Jenoptik ProgRes CapturePro 2.5 Camera
- Fisher Scientific, Fisherfinest Premium Cover Glass
- VWR VistaVision Microscope Slides
- Electrodes
- Spacers
- Pipettes
- Aluminum Tray
- 250ml flaks
- Beaker
- Funnel

Reagents:

- EMD® Magnesium sulfate GR, Powder, 500 g
- 15% CO₂ algae culture
- Deionized water

Procedure:

To set up the reactor, in order from left to right, 9 spacers (so that the hydraulic jack could reach to pressure enough the reactor so that the sample not shed), the film that contained the inlet tube, an electrode (negative), a spacer, the spacer with the exhaust tube, another electrode (positive) and finally the film that contained the outlet tube (which was plugged to not waste volume) were placed inside of it.

285 ml algae sample (reactor volume) were taken from the flask and poured into the reactor using a funnel. Using pincers, the power supply was connected to each electrode, negative on the left and positive on the right.

For power supply, BK Precision 1791 was used. Two different modes were applied:

- **Constant Voltage (CV) mode:**

The “POWER ON” switch was pressed and the “OUTPUT ON/OFF” switch was kept in the OFF position. Then, the “LIMIT” button switch was pressed and the voltage was adjusted; after that, the “OUPUT” switch was pressed to ON position and the CV LED light turned on.

- **Constant Current Voltage (CC) mode:**

The power supply was turned off, a short circuit in the output terminals of the power supply was done and then the supply was turned on. Then the “OUTPUT ON/OFF” switch was kept in the OFF position, the “LIMIT” button switch was pressed and the current was adjusted; after that, the “OUPUT” switch was pressed to ON position and the CC LED light turned on; finally, the short circuit was removed.

The conductivity of the effluent of a regular wastewater treatment plant is around 1264 $\mu\text{S}/\text{cm}$ (De Grau, 2015). However, in order to work with constant current, is necessary to increase the conductivity of the sample to be treated. For this purpose, 1g/300ml of magnesium sulfate were added to the algae culture.

For both modes, 30 seconds were allowed for charging the electrodes.

After turning the power supply off, the hydraulic jack was released and the sample fell into the tray, poured into the flask and taken to further analysis in the microscope, to check if the algae cell wall was broken.

For cell wall analysis pictures were taken at all times.



Figure 57. Cell wall analysis equipment.

Same procedure was done, for different detention times.

Appendix B: Experimental results.

Table 13. pH values for flask 3.

Flask 3 (15% CO ₂)					
Time (Days)	pH	{H ⁺ }	Time (Days)	pH	{H ⁺ }
0	7	0.0000001	20	9.1	7.94328E-10
1	6	0.000001	21	8.1	7.94328E-09
2	6	0.000001	22	9.1	7.94328E-10
3	6	0.000001	23	9.1	7.94328E-10
4	8.5	3.16228E-09	24	9.2	6.30957E-10
5	8.9	1.25893E-09	25	9.1	7.94328E-10
6	5.8	1.58489E-06	26	9.1	7.94328E-10
7	5.6	2.51189E-06	27	9.1	7.94328E-10
8	8.9	1.25893E-09	28	9.2	6.30957E-10
9	8.4	3.98107E-09	29	9.1	7.94328E-10
10	8.1	7.94328E-09	30	8.7	1.99526E-09
11	8.7	1.99526E-09	31	9.2	6.30957E-10
12	8.9	1.25893E-09	32	9.1	7.94328E-10
13	9	0.000000001	33	6.3	5.01187E-07
14	5.9	1.25893E-06	34	9.3	5.01187E-10
15	6.5	3.16228E-07	35	9.3	5.01187E-10
16	9	0.000000001	36	9.2	6.30957E-10
17	9	0.000000001	37	9.3	5.01187E-10
18	9	0.000000001	38	9.3	5.01187E-10
19	9.1	7.94328E-10	39	9.3	5.01187E-10
20	9.1	7.94328E-10	40	8.9	1.25893E-09
				Average {H⁺}	2.2735E-07

Table 14. Non-linear regression on data turbidity vs. time for flask 0.

Flask 0 (0% CO ₂)				
Days	Turbidity	Predicted	(y-f) ²	(y - y _{avg}) ²
0	5.4	2.018865485	11.43207061	825.1698179
2	5.22	4.006443489	1.472719407	835.5434948
3	6.09	5.643942331	0.198967444	786.0043564
4	8.57	7.950670417	0.383569133	653.097341
5	11.5	11.2000924	0.089944571	511.9254333
6	15.6	15.77737584	0.031462187	343.2041256
7	22.4	22.22497759	0.030632843	137.4936641
8	27.4	31.30679352	15.26303559	45.23597175
9	46.4	44.09839077	5.297405025	150.656741
	16.50888889		34.1998068	4288.330946

Table 15. Non-linear regression on data turbidity vs. time for flask 1.

Flask 1 (5% CO ₂)				
Days	Turbidity	Predicted	(y-f) ²	(y - y _{avg}) ²
0		0.469174946	0.22012513	1164.568126
2	3.19	1.001683491	4.78872914	957.0218179
3	2.61	1.458584668	1.32575727	993.2437102
4	6.02	2.116050023	15.2408254	789.9342641
5	5.61	3.053644017	6.53495591	813.1490948
6	15.4	4.373703085	121.579224	350.6544333
7	8.29	6.199108749	4.37182623	667.4869717
8	7.15	8.661510521	2.28466405	727.6921256
9	10.4	11.87440739	2.17387716	562.9121256
10	11.5	15.88916593	19.2647776	511.9254333
11	16.9	20.64344742	14.0133986	296.7271256
12	22	25.92799645	15.4291561	147.0342794
13	36.9	31.4040326	30.2056577	7.696356361
14	37.7	36.68113177	1.03809247	12.77512559
16	40	45.42170578	29.3948936	34.50658713
17	50.3	48.61915377	2.82524405	261.605741
18	62.5	51.06789673	130.692985	805.0969717
19	51.1	52.88215941	3.17609218	288.1245102
20	58.7	54.19362092	20.3074524	603.8928179
21	53.7	55.1248335	2.03015051	383.1505102
22	46.7	55.77768794	82.4044182	158.1112794
23	54.2	56.23131872	4.12625573	402.974741
24	55.8	56.54456654	0.55437934	469.7722794
25	67.8	56.75994733	121.882763	1133.953818
26	49.1	56.90760008	60.9586191	224.2275871
27	52.1	57.00861726	24.0945234	323.0729717
28	61.6	57.07763268	20.4518062	754.8333564
	34.12576923		741.370649	13846.14416

Table 16. Non-linear regression on data turbidity vs. time for flask 2.

Flask 2 (10% CO ₂)				
Days	Turbidity	Predicted	(y-f)^2	(y - y _{avg})^2
0		0.001638461	2.68455E-06	752.5877778
2	3.87	0.009536704	14.90317686	555.2306778
3	3.36	0.023002814	11.13555022	579.5253778
4	6.05	0.055458367	35.9345294	457.2469444
5	4.64	0.133561028	20.30799221	519.5360444
6	5.05	0.32081546	22.36518641	501.0136111
7	5.75	0.765802076	24.84222894	470.1669444
8	7.13	1.801336636	28.39465325	412.2253444
9	8.6	4.09800873	20.26792539	354.6944444
10	8.75	8.690019973	0.003597604	349.0669444
11	13.9	16.22534727	5.407239904	183.1511111
12	19.2	25.32774889	37.5493064	67.7877778
13	35	33.00071773	3.997129593	57.25444444
14	44.5	37.73917915	45.70869852	291.2711111
15	48.2	40.12715769	65.17078298	431.2544444
16	39.4	41.20783446	3.268265444	143.2011111
17	37.3	41.67298127	19.1229652	97.35111111
18	43.8	41.86885645	3.729315402	267.8677778
19	46	41.9505788	16.39781203	344.7211111
21	44.8	41.99863532	7.84764405	301.6011111
22	35.4	41.99863532	7.84764405	301.6011111
23	43.5	42.00447887	43.61914119	63.4677778
24	41.1	42.00690124	2.229343901	258.1377778
25	37.6	42.00790529	0.824292013	186.7777778
26	36.5	42.00832144	19.43329788	103.3611111
27	36.1	42.00849391	30.34350518	82.20444444
28	46.8	42.0085654	34.91114504	75.11111111
31	38.4	42.00859502	22.95756165	375.0677778
	27.43333333		548.5199334	8582.484111

Table 17. Non-linear regression on data turbidity vs. time for flask 3.

Days	Flask 3 (15% CO ₂)			
	Turbidity	Predicted	(y-f) ²	(y - y _{avg}) ²
0		6.043618306	36.52532223	21870.97246
2	3.58	8.822727515	27.4861918	20824.90807
3	4.4	10.64345332	38.98070933	20588.91473
4	6.49	12.82308451	40.10795947	19993.50141
5	10.2	15.42486504	27.29921469	18958.08954
6	12.8	18.51990053	32.71726213	18248.86997
7	17.3	22.18668627	23.87970274	17053.32457
8	23.3	26.50986547	10.30323636	15522.26403
9	27.1	31.57794595	20.05199997	14589.83235
10	29.6	37.47969691	62.08962343	13992.14046
11	70.7	44.29899558	697.0130346	5958.045757
12	70.8	52.10802553	349.3899096	5942.618081
13	75.2	60.95897105	202.8069057	5283.600351
14	82.2	70.8747124	128.2621392	4314.963054
15	91.9	81.83947482	101.2141669	3134.698513
16	92.3	93.79082913	2.222571503	3090.067811
17	103	106.614736	13.06631603	2014.966513
18	125	120.1452892	23.56821648	523.8778648
19	119	134.1703122	230.1383726	834.5384053
20	118	148.4429862	926.7754097	893.3151621
21	148	162.6984432	216.0442319	0.012459386
22	174	176.6730849	7.145383106	681.8167837
23	199	190.1237077	78.78856554	2612.397865
24	192	202.8435595	117.5827825	1945.835162
25	220	214.6732257	28.37452481	5200.085973
26	219	225.5054367	42.32070693	5056.86273
27	215	235.284127	411.4458079	4503.969757
28	294	243.9989893	2500.101067	21348.60597
29	294	251.6772106	1791.2185	21348.60597
30	224	258.3740569	1181.575789	5792.978946
31	258	264.1636539	37.99062942	12124.56922
32	304	269.1308551	1215.857268	24370.83841
33	319	273.3646505	2082.585122	29279.18705
34	241	276.9532223	1292.634191	8669.774081
35	282	279.9805255	4.078277077	17985.92705
36	241	282.5241555	1724.255488	8669.774081
37	260	284.654219	607.8305145	12569.0157
38	305	286.4329438	344.7355747	24684.06165
	147.8883784		16678.46269	420477.828

Table 18. Non-linear regression on data turbidity vs. time for flask 4.

Days	Flask 4 (20% CO ₂)			
	Turbidity	Predicted	(y-f) ²	(y - y _{avg}) ²
0		11.04624928	122.019623	14860.01634
2	3.94	13.96324167	100.465374	13914.9548
3	4.49	15.6878602	125.392073	13785.49947
4	6.5	17.61581864	123.561424	13317.54467
5	6.98	19.76858882	163.548004	13206.98947
6	8.55	22.16926869	185.48448	12848.60034
7	13.4	24.84253715	130.931656	11772.61167
8	29.4	27.81455466	2.51363694	8556.558336
9	46.1	31.11279659	224.616266	5745.892669
10	23.3	34.76580558	131.464697	9722.288669
11	80.6	38.80284825	1747.00189	1705.827669
12	64.6	43.25346265	455.674657	3283.481003
13	83	48.14688375	1214.73971	1513.339669
14	48.6	53.51133826	24.1212435	5373.134336
15	66.4	59.3732047	49.3758522	3080.435003
16	82.2	65.75604267	270.403733	1576.222336
17	73.3	72.67950501	0.38501403	2362.122003
18	92	80.15815908	140.229196	894.1096694
19	96.1	88.20025745	62.4059324	665.7260028
20	69.1	96.80651366	767.650899	2788.016003
21	81.7	105.9689529	588.982073	1616.174003
22	90.2	115.6699193	648.71679	1004.995669
23	106	125.8813296	395.267267	252.8630028
24	131	136.5642599	30.9609878	82.77966944
25	124	147.6689461	560.219009	4.403002778
26	164	159.1352563	23.6657309	1772.269669
27	176	170.8936642	26.0746655	2926.629669
28	233	182.8667148	2513.34628	12342.83967
30	164	207.1190876	1859.25571	1772.269669
31	256	219.2226695	1352.57204	17982.363
32	251	231.1944643	392.259243	16666.37967
34	262	254.4149727	57.532639	19627.543
36	236	276.1965122	1615.75959	13018.42967
37	273	286.4043654	179.677013	22830.70634
38	320	296.1015336	571.136694	39242.94967
39	343	305.2600106	1424.3068	48884.473
40	279	313.8622134	1215.37392	24679.88634
	121.901667		19497.0918	365681.3248

Table 19. Correlation between turbidity and chlorophyll concentration.

CO ₂ %	Pigment concentration per volume of culture (µg/L = mg/m ³)	Turbidity (NTU)
5	1050.6552	125
10	901.3548	52
15	5559.0264	195
20	5149.56	279

Table 20. Daily measurements.

Date	Day	Flask	pCO ₂	Temperature (°C)	Conductivity (µS/cm)	pH	Turbidity (NTU)
8/8/2016	0	0	0	22.6	1178	8.6	5.4
		1	5	18.2	1018	7	-
		2	10	18.2	1018	7	-
		3	15	18.2	1018	7	-
		4	20	18.2	1018	7	-
8/9/2016	1	0	0	23.4	1436	8.7	3.11
		1	5	22.4	1192	6.6	-
		2	10	22.8	968	6.1	-
		3	15	22.6	1045	6	-
		4	20	22.5	1062	6	-
8/10/2016	2	0	0	24.9	1555	8.7	5.22
		1	5	22.1	1654	6.9	3.19
		2	10	22.9	1052	6.2	3.87
		3	15	23.1	1091	6	3.58
		4	20	23.1	1111	5.9	3.94
8/11/2016	3	0	0	24.1	1946	8.8	6.09
		1	5	22.1	1517	7.2	2.61
		2	10	22.9	1067	6.3	3.36
		3	15	23.1	1096	6	4.4
		4	20	23.1	1123	5.8	4.49
8/12/2016	4	0	0	24.2	1789	8.9	8.57
		1	5	22.1	1869	8.7	6.02
		2	10	22.6	1265	8.7	6.05
		3	15	23	1213	8.5	6.49
		4	20	23	1269	8.5	6.5
8/13/2016	5	0	0	24	2122	8.9	11.5
		1	5	24.7	1738	8.9	5.61
		2	10	25.2	1253	8.7	4.64
		3	15	25.4	1309	8.9	10.2
		4	20	25.6	1382	8.8	6.98
8/14/2016	6	0	0	24.5	2403	9	15.6
		1	5	25	1753	5.9	15.4
		2	10	25.5	1282	5.8	5.05
		3	15	25.9	1398	5.8	12.8
		4	20	25.6	1460	5.7	8.55
8/15/2016	7	0	0	25	2350	9	22.4
		1	5	25.6	1326	5.6	8.29
		2	10	25.8	1358	5.6	5.75
		3	15	25.9	1443	5.6	17.3
		4	20	26	1598	5.6	13.4
8/16/2016	8	0	0	24.1	2905	9	27.4
		1	5	25.1	1353	8.8	7.15
		2	10	25.5	1399	8.8	7.13
		3	15	25.7	1523	8.9	23.3
		4	20	25.8	1693	8.8	29.4
8/17/2016	9	0	0	23.8	3660	9.2	46.4
		1	5	24.8	1486	8.9	10.4
		2	10	25.1	1464	8.8	8.6
		3	15	25.2	1638	8.4	27.1
		4	20	25.1	1863	9	46.1
8/18/2016	10	0	0	23.8	3690	9.1	41.6
		1	5	23.6	1541	8.8	11.5
		2	10	24.6	1485	8.1	8.75
		3	15	24.2	1745	8.1	29.6
		4	20	24	2110	8.7	23.3

(Table 20 continued)

8/19/2016	11	0	0	24	3680	9.1	39
		1	5	25.1	1649	8.4	16.9
		2	10	25.3	1654	8.3	13.9
		3	15	24.8	1853	8.7	70.7
		4	20	24.8	2312	8.9	80.6
8/20/2016	12	0	0	24.8	3460	9.1	33.2
		1	5	24.9	1607	8.6	22
		2	10	25.1	1645	8.6	19.2
		3	15	25.3	1793	8.9	70.8
		4	20	25.4	2070	8.8	64.6
8/21/2016	13	0	0	23.3	4040	9.2	26.8
		1	5	24	1891	8.8	36.9
		2	10	24.9	1732	8.7	35
		3	15	25.3	1894	9	75.2
		4	20	25.2	2247	9	83
8/22/2016	14	0	0	23.9	4630	9.3	34.7
		1	5	25.4	1944	6.1	37.7
		2	10	25.6	1794	5.9	44.5
		3	15	25.8	2082	5.9	82.2
		4	20	25.5	2542	6	48.6
8/23/2016	15	0	0	25.4	3630	8.8	12.1
		1	5	24	2795	8.9	94
		2	10	25.1	2000	8.7	48.2
		3	15	25.6	2260	6.5	91.9
		4	20	25.6	2891	8	66.4
8/24/2016	16	0	0	23.5	4980	9.3	20.7
		1	5	24	2193	8.8	40
		2	10	25.3	1911	8.8	39.4
		3	15	25.4	2109	9	92.3
		4	20	25.5	2425	9	82.2
8/25/2016	17	0	0	25.4	3900	9.2	12.6
		1	5	24.3	2508	8.9	50.3
		2	10	25	1942	8.8	37.3
		3	15	25.4	2263	9	103
		4	20	25.5	2583	9	73.3
8/26/2016	18	0	0	25.8	3910	8.8	11.7
		1	5	24.3	2833	8.9	62.5
		2	10	25.1	1990	8.8	43.8
		3	15	25.3	2473	9	125
		4	20	25.5	2841	9	92
8/27/2016	19	0	0	23.2	4840	9.2	19.4
		1	5	24.3	2729	9.1	51.1
		2	10	25.1	1809	8.8	46
		3	15	25.4	2168	9.1	119
		4	20	25.5	2719	9	96.1
8/28/2016	20	0	0	24.9	4630	9.1	10.1
		1	5	24.6	2980	8.9	58.7
		2	10	24.8	2014	8.8	56.7
		3	15	25	2322	9.1	118
		4	20	25.2	2763	9.2	69.1

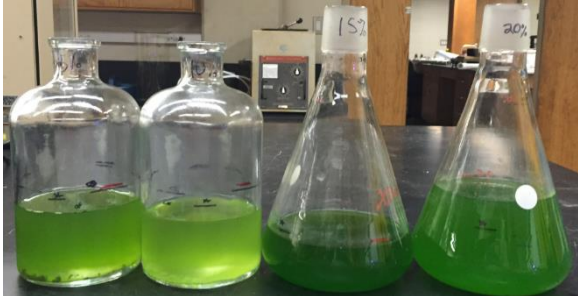
(Table 20 continued)

8/29/2016	21	0	0	24.6	4640	9.3	6.79
		1	5	24.1	3100	9	53.7
		2	10	25.1	1661	8.9	44.8
		3	15	23.9	3080	8.1	148
		4	20	24.9	2783	9	81.7
8/30/2016	22	0	0	23.7	6220	9.3	14.2
		1	5	24.2	1813	8.8	46.7
		2	10	25.2	2803	8.9	35.4
		3	15	25.6	2439	9.1	174
		4	20	25.5	2923	9.1	90.2
8/31/2016	23	0	0	24.1	5470	9.3	17.1
		1	5	24.4	3200	9	54.2
		2	10	25.2	1849	8.9	43.5
		3	15	25.4	2648	9.1	199
		4	20	25.5	3130	9.1	106
9/1/2016	24	0	0	23.5	6880	9.4	11.1
		1	5	24.1	3400	9.1	55.8
		2	10	24.9	1801	8.8	41.1
		3	15	24.1	3400	9.2	192
		4	20	25.6	3380	9.2	131
9/2/2016	25	0	0	24.4	5270	9.3	8.85
		1	5	24.3	4410	9	67.8
		2	10	24.6	2019	8.9	37.6
		3	15	25.5	2735	9.1	220
		4	20	25.4	3590	9.1	124
9/3/2016	26	0	0	22.6	6230	9.3	6.83
		1	5	24.2	3560	9	49.1
		2	10	24.9	1860	8.8	36.5
		3	15	25.5	2724	9.1	219
		4	20	25.6	3800	9.1	164
9/4/2016	27	0	0	23.4	7030	9.2	13.9
		1	5	23.9	3590	9	52.1
		2	10	24.8	1930	8.9	36.1
		3	15	25.4	2848	9.1	215
		4	20	25.5	4140	9.1	176
9/5/2016	28	0	0	20.9	7820	9.2	15.1
		1	5	23	4240	9.1	61.6
		2	10	24.6	2510	8.8	46.8
		3	15	25.2	3100	9.2	294
		4	20	24.8	4560	9.2	233
9/6/2016	29	0	0	20.7	6440	9.3	12.8
		1	5	23.8	5390	8.9	83.6
		2	10	24.4	2441	8.8	57.4
		3	15	25.2	3330	9.1	294
		4	20	25.4	4940	9.2	291
9/7/2016	30	0	0	20.1	7910	9.4	18
		1	5	24.2	3380	9	33.2
		2	10	25.2	1866	8.7	30.1
		3	15	25.6	2880	8.7	224
		4	20	25.6	4510	7	164

(Table 20 continued)

9/8/2016	31	1	5	23.9	4040	9.1	69.1
		2	10	24.6	2002	8.9	38.4
		3	15	25.3	3030	9.2	258
		4	20	25.5	4800	9.2	256
9/9/2016	32	1	5	23.1	3980	9	75.6
		2	10	24.2	2097	8.8	49.5
		3	15	25.1	3210	9.1	304
		4	20	25.3	4710	9.2	251
9/10/2016	33	1	5	24.1	3.52	9	80.9
		2	10	25	2244	6.9	36.5
		3	15	24.9	3580	6.3	319
		4	20	25.4	5150	6.6	128
9/11/2016	34	1	5	23.4	3060	9.1	57.8
		2	10	23.8	1819	8.9	45.3
		3	15	24.7	2990	9.3	241
		4	20	25.3	5520	9.3	262
9/12/2016	35	1	5	23.5	3290	9	85.1
		2	10	24.6	1895	8.9	52
		3	15	25.2	3070	9.3	282
		4	20	25.4	6060	9.3	362
9/13/2016	36	1	5	23.3	3050	9.1	83
		2	10	24.8	1740	8.9	38.9
		3	15	25.4	2811	9.2	241
		4	20	25.6	4750	9.2	236
9/14/2016	37	1	5	24.6	3350	9.1	97.1
		2	10	25.1	1826	8.9	45.3
		3	15	25.5	2976	9.3	260
		4	20	25.6	4970	9.4	273
9/15/2016	38	1	5	24.4	3730	9.2	128
		2	10	25	1943	8.9	57.5
		3	15	25.4	3230	9.3	305
		4	20	25.6	5170	9.3	320
9/16/2016	39	1	5	24.5	3160	9.2	95.3
		2	10	25.1	1811	9	44.3
		3	15	25.5	2522	9.3	186
		4	20	25.5	5450	9.3	343
9/17/2016	40	1	5	24.2	3810	9.2	125
		2	10	25.3	1965	8.9	52
		3	15	25.6	2699	8.9	195
		4	20	25.3	5000	9.1	279

Table 21. Algae culture progress.

Week	Progress
Initial	 Four glass vessels containing clear, colorless liquid. From left to right: two round-bottom flasks and two Erlenmeyer flasks. The two Erlenmeyer flasks on the right have white labels with '15%' and '20%' written on them.
1	 Four glass vessels. The two round-bottom flasks on the left contain clear liquid. The two Erlenmeyer flasks on the right contain a pale yellow-green liquid. The Erlenmeyer flasks have white labels with '15%' and '20%' written on them.
2	 Four glass vessels. The two round-bottom flasks on the left contain a light green liquid. The two Erlenmeyer flasks on the right contain a medium green liquid. The Erlenmeyer flasks have white labels with '15%' and '20%' written on them.
3	 Four glass vessels. The two round-bottom flasks on the left contain a dark green liquid. The two Erlenmeyer flasks on the right contain a very dark green liquid. The Erlenmeyer flasks have white labels with '15%' and '20%' written on them.

(Table 21 continued)

Week	Progress
4	
5	
6	

Vita

Alicia Eugenia Simosa Mellado, was born in Maturin, Venezuela in 1992. She graduated from Universidad Católica Andrés Bello – Núcleo Guayana with a bachelor's degree in Civil Engineering in October of 2014.

10 months after her graduation she pursued a Master's degree in Civil and Environmental Engineering at the University of New Orleans and became a member of Professor Enrique La Motta's research groups in 2015.